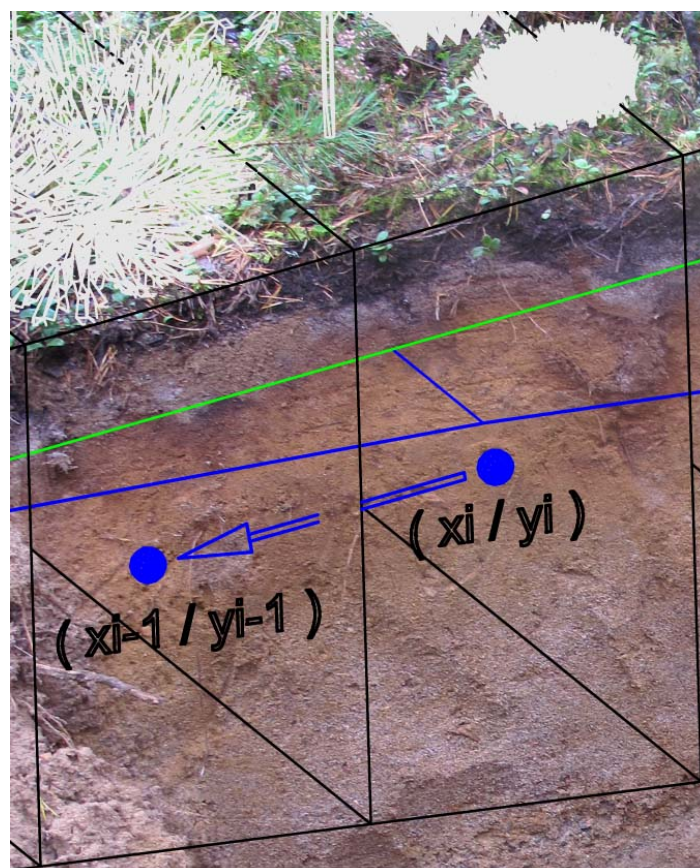


Quantifying hillslope flowpaths and residence times of water implied by the transmissivity feedback hypothesis: An application of the MIPS concept

Ulrich Tschiesche



Department of Aquatic Sciences and Assessment
Uppsala 2012

Master's thesis • 30 hec •

Quantifying hillslope flowpaths and residence times of water implied by the transmissivity feedback hypothesis: An application of the MIPS concept

Ulrich Tschiesche

Supervisor: Kevin Bishop

Co-supervisor: Josef Fürst

University of Natural Resources and Life Sciences, Vienna; Department of Water, Atmosphere and Environment; Institute of Water Management, Hydrology and Hydraulic Engineering

Examiner: Stephan Köhler

Credits: 30 hec

Level: Advanced, E

Course title: Independent Project in Environmental Science - Master's thesis

Course code: EX0431

Programme/education: EnvEuro – Environmental Science in Europe

Year of Publication 2012

Place of publication: Uppsala

Online publication: <http://stud.epsilon.slu.se>

Key Words: transmissivity feedback, hillslope model, particle tracking, tracer experiment, run-off processes

Contents

Abstract	i
1. Introduction	1
2. Materials and methods	5
2.1. Study site description	5
2.2. Experimental design	6
2.3. Data used	7
2.3.1. Precipitation and soil infiltration	7
2.3.2. Runoff.....	8
2.3.3. Groundwater level	9
2.3.4. Evapotranspiration.....	10
2.3.5. Soil properties.....	11
2.4. Model description.....	13
2.4.1. Slope set-up	14
2.4.2. Defining initial conditions	17
2.4.3. Defining the input boundary conditions	21
2.4.4. Defining the step equations	22
2.4.5. Defining the transition probability matrices.....	23
2.4.6. Defining evapotranspiration	24
2.5. Model settings	25
2.6. Parameter sensitivity analysis.....	28
3. Results	29
3.1 Model performance	29
3.2 Drainage and stream runoff.....	30
3.2.1. The influence of changing the surface saturated hydraulic conductivity	32
3.2.2. The influence of changing the f – value	33

3.2.3. Separation of pre-event and event water	34
3.3. Groundwater level	35
3.4. Water storage.....	37
3.5. Evapotranspiration.....	40
3.6. Velocity distribution	42
3.7. Unsaturated zone initial flux	44
3.8. Slope geometry	47
4. Discussion	50
4.1. Goodness – of – fit	50
4.2. Transmissivity feedback and discharge.....	51
4.3. Groundwater levels and water storage	52
4.4. The influence of evapotranspiration	53
4.5. Particle velocities and their representation.....	53
4.6. The steady state assumption	54
5. Conclusion	55
Acknowledgements	56
Appendices.....	57
Register of Figures	58
Register of Tables	61
References.....	62

Abstract

The Multiple Interacting Pathways (MIPS) model is a physically based approach for simulating groundwater flow within a hillslope. The MIPS model covers the soil heterogeneities and preferential flow pathways by representing water as particles with a specific volume and through application of velocity distributions and transition probability matrices. To test the underlying assumptions, the model was applied to a slope in the Svartberget catchment in northern Sweden. Several model simulations have been conducted assuming different parameter combinations for a one-year and three-year period. The model is able to reproduce runoff with reasonable success according to transmissivity feedback hypothesis. The steady state at initial time and linear decrease of porosity with depth assumption was analyzed and discussed. Evapotranspiration was incorporated into the model using a transition probability matrix which led to a better model performance.

Keywords: transmissivity feedback, hillslope model, particle tracking, tracer experiment, run-off processes

1. Introduction

The relationship between rainfall and runoff keeps hydrologists busy since many years. Several attempts have been undertaken to simulate those interactions and different kinds of models have been developed.

In general, there are two main intentions why scientists develop these models. On one hand they are testing their assumptions about a real world natural state and on the other they intend to predict the behavior of a real world system under a set of naturally occurring circumstances (Beven, 1989).

Furthermore, they are used to solve many engineering design problems. The correct prediction of peak discharge rates is essential for the design of stormwater runoff facilities such as pipe systems, storm inlets and culverts, as well as small open channels (McCuen, 1998). For design projects where the catchment or storage within the stream is significant, such as storage in manmade structures like dams or storage in natural reservoirs or streams, the overall performance of the prediction is essential.

In the last years hydrological models are increasingly used also for studying the impacts of climate change on water resources. Key issues here are the impacts on the catchment hydrology, especially water balance changes, and the impacts on extreme events such as floods, low flows or droughts.

In terms of rainfall, runoff modeling different approaches have been developed which intend to predict e.g. the discharge in a stream due to certain precipitation events.

Models which generalize certain catchment properties like water storage, soil properties or land cover to average values and assume the catchment as a single unit are called lumped models.

Whereas conceptual models basically divert the catchment area into elements or grid squares where each elements or grid cell has certain averaged properties assigned. Then transition equations are solved for each element or grid cell.

In general there is a strong correspondence between distributed and “physically-based” models and lumped and “explicit soil moisture accounting” (ESMA) models (Beven, 1989). But the definitions and interrelations are blurry as elements of lumped models are often used within current available distributed models. Therefore currently available distributed models can be seen as lumped conceptual models at the element scale (Beven, 1989, 2006).

There are several assumptions that can be made for lumped conceptual models. The equations used in lumped conceptual models are only approximations of the real natural processes. Therefore, a certain error has to be considered. Another important assumption is that the used average values can't reproduce local and spatial heterogeneities (Beven, 1989).

By using only effective parameter values each grid cell is treated as homogeneous and boundary conditions need to be defined. This leads to high computation demands and groundwater flow can't be appropriately reproduced. To overcome the problems that occur from the effects of heterogeneity and the use of small scale physics equations, more complex equations and concepts have been developed.

One of the latest developed concepts which is based on global balance laws for mass, momentum and energy formulated for representative hydrological control volumes is the REW (Representative Elementary Watersheds) concept by Reggiani et al. (2005).

Other concepts to overcome the former mentioned problems – starting with the usage of average values as parameters – are using probability functions for the account of soil heterogeneity. Stochastic models have been found a very useful and valuable tool in terms of understanding velocity distributions. Earlier stochastic models are the MIPS (Multiple Interacting Pathways) model by Beven (1989) which at that time was conducted only for steady state conditions and the SAMP (Subsystems And Moving Packets) model by Ewen (1996).

Davies et al. (2011) further developed the MIPS model for dynamic conditions. The model was tested within a tracer experiment in the Gårdsjön catchment.

The first underlying idea of MIPS is that model parameters or components are not calibrated to whatever data is available, but to use more or less reliable data from physical properties - like hydraulic conductivity or soil porosity as a foundation and starting point for understanding and simulating groundwater flow processes within a hillslope. Water is treated as water particles with a pre-defined volume and assigned velocities depending on its current spatial and temporal state and position. At the time a particle enters the soil it moves vertically through the unsaturated zone until it reaches the groundwater-saturated zone. From there on it follows a unique hydraulic gradient to the outlet of the slope. The time a particle stays within the slope strongly depends on its velocity, which is randomly assigned according to an exponential distribution between a minimum and a maximum value.

The second basic idea behind MIPS is that soil heterogeneities are represented without the need of cost and labor intensive soil investigations. This is done by the previously mentioned randomly assigned velocities, but also through the use of 'transition probability matrices' which represent probabilities of particles changing from one pathway or condition to another. These probability matrices can additionally be used to simulate evapotranspiration, or the leakage into bedrock.

The main purpose of this work is to use MIPS as a tool first for rainfall-runoff simulations and second to analyze the model's outputs like: runoff, groundwater tables, water storage or particle velocities in order to examine the model's limitations and underlying assumptions. In the following work the model is applied to an experimental site in northern Sweden which is different to Gårdsjön where it was first tested. The different local conditions and properties of the slope enable additional model testing and discussion of the following key issues:

The effect of changing basic model inputs like saturated hydraulic conductivity and porosity on the model's outputs, specifically:

- How and to which extent do changes in soil properties affect simulated groundwater flow in terms of groundwater table, water storage and runoff prediction?
- Is the model's performance in terms of runoff prediction satisfying?
- How can the interrelation between discharge and groundwater level be described and incorporated into the model?
- Does the steady state at initial time assumption provide reasonable results in terms of predicting runoff, groundwater levels or groundwater storage?

So far, evapotranspiration was not considered in the studies of Davies et al. (2011). Since this work intends to analyze the concept for a whole hydrologic year and even longer time periods evapotranspiration has a significant influence on the water balance and must be considered.

Therefore, one part of this work will deal with the questions:

- How was evapotranspiration taken into account?
- How and to what extent does evapotranspiration influence the results?

By applying the MIPS concept to the site in northern Sweden, we leave the thought of soil as grid element box behind and move on to a state where soil is heterogeneous and exhibits diverse properties. The concept itself is probably not the only valid solution to the problem of

soil heterogeneity but can be used as an important tool for understanding groundwater fluxes as well as rainfall runoff relationships.

2. Materials and methods

2.1. Study site description

The study site is located in the 50 ha Svarthberget catchment (see Figure 1a) within the Svarthberget long term ecological research site in the province of Vindeln, northern Sweden ($64^{\circ}14'N$, $10^{\circ}46'E$). The research park was established 1923. Starting in 1979 monitoring stations have been installed to collect long-term climatic, soil and water budget data (Rodhe, 2003).

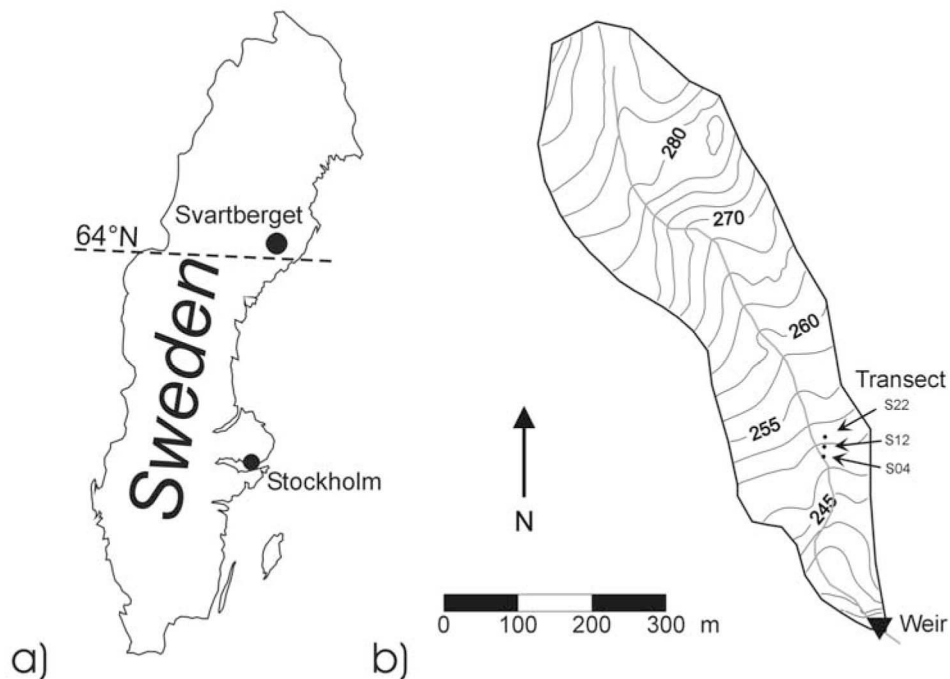


Figure 1: a) Location of the catchment and b) the studied hillslope within the catchment (from Laudon, 2004)

The Svarthberget catchment is divided into two sub-catchments. The larger one is called Kallkällbäcken which drains about 41 ha and the second one is called Västrabäcken (engl. Western brook) which drains about 13 ha. Both streams were artificially influenced when the ditches were deepened in the 1930s in order to improve the drainage of forest soils.

On the higher well drained soil the catchment is afforested with Scots Pine (*Pinus sylvestris*) and Norway Spruce (*Picea abies*) in wetter and lower situated areas. Other present local vegetation are a mix of heather (*Calluna vulgaris*), berries (*Vaccinium myrtillus*) and grasses (*Deschampsia flexuosa*) for the field layer and a mix of lichen (*Cladonia spp.*), mesic mosses (*Hylocomium splendens*) and wet mosses (*Sphagnum spp.*) on the bottom layer (Rodhe, 2003).

Building up on gneissic bedrock a 10 - 15 m thick layer of glacial till is overlain by less compacted ablation till in which sandy material is dominant. The top layers in most of the catchment are ferric- to orthic podzols. In the vicinity of the two tributaries the podzols give space to a 10 - 20 m wide and 0.2 – 0.8 m deep zone of riparian peat on both sides.

2.2. Experimental design

The S-transect in Svartberget is one of the most studied hydrological research sites in northern Sweden. Earlier research at the transect was conducted by Bishop (1993), Bishop et al (1996), Nyberg et al (2001), Stähli et al (2001), Lindström et al (2002), Laudon et al (2002, 2004) and Seibert et al (2009) among others. At an oblique angle the transect extends from the stream to the watershed divide of Västrabäcken (Figure 2).

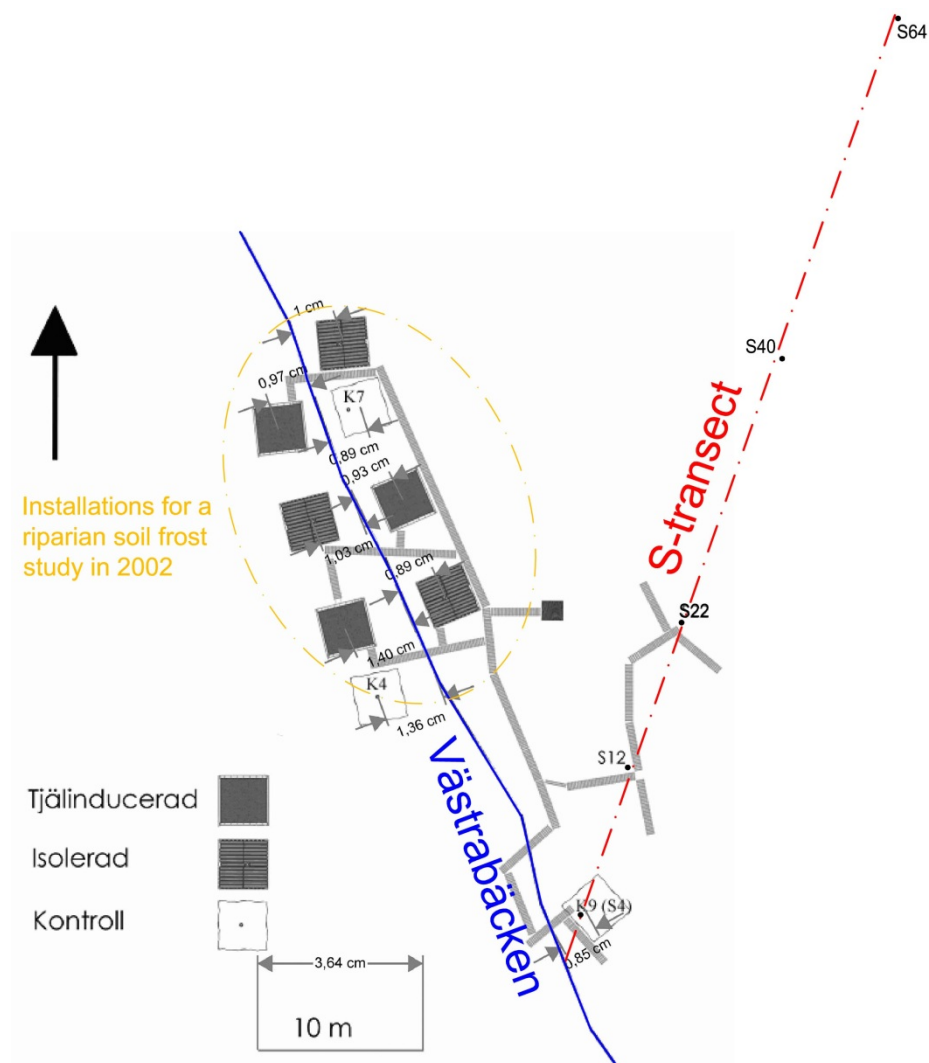


Figure 2: Overview of measurement locations along Västrabäcken and the S-transect (after Bishop, 1993)

Instruments such as suction Lysimeters, Piezometers, TDRs, temperature probes, soil gas probes and perforated groundwater tubes are situated along the transect in distances 4 m (S4), 12 m (S12), 22 m (S22), 40 m (S40) and 64 m (S64). The location S64 is the upmost of the slope and lies close to the watershed boundary of Västrabäcken catchment.

2.3. Data used

2.3.1. Precipitation and soil infiltration

Reasonable meteorological data like air temperature and precipitation were measured at an open field, 1300 m south-west of the transect (Nyberg et al, 2001).

Stähli et al (2001) created soil infiltration data by applying the COUP model to the S-transect. Soil infiltration into frozen soil was calculated using Richards' equation for water flow, Fourier equation for heat flow and a surface energy balance equation (Stähli et al, 2001). In the model used there - input parameters, like the heat transfer coefficient and the damping ice content, have been found crucial for estimating snowmelt infiltration. Different settings of those parameters resulted in different water infiltration estimates and model performances.

Even though these soil infiltration values contain errors they have been found more relevant for the purpose of this work and were therefore chosen as model input. Another advantage of directly using soil infiltration data is that other important hydrological components, as there are: interception, surface retention, overland flow or snow accumulation and melt, don't need to be measured or calculated separately. Since soil infiltration data isn't always available for different experimental sites the above mentioned hydrological components should be incorporated in the future applications of the MIPS model.

Figure 3 shows a soil infiltration, discharge and air temperature time series for the investigated time period November 1995 to June 1998.

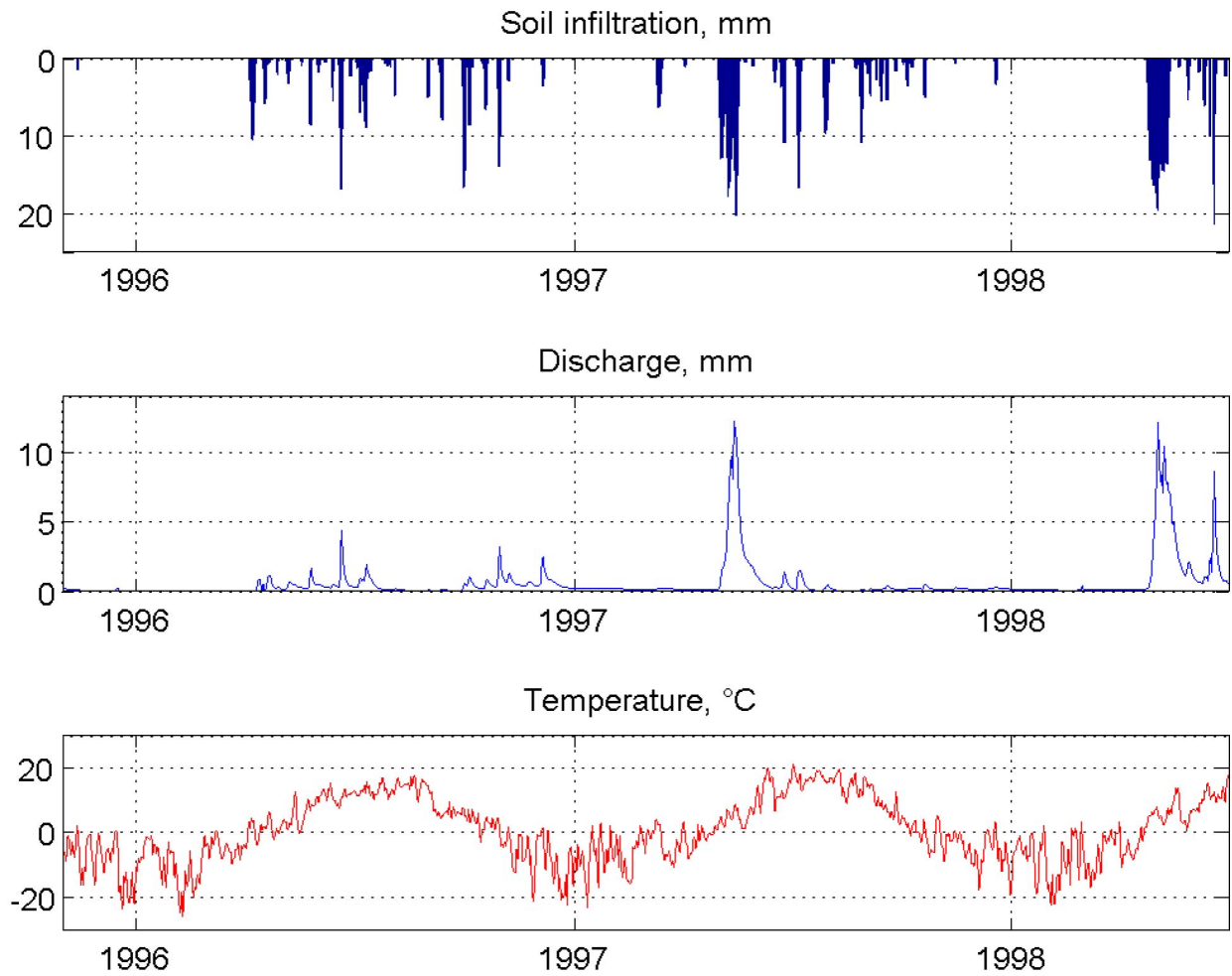


Figure 3: Daily soil infiltration, discharge and air temperature during the investigated time period

In northern Sweden, the winter season lasts from November until the main snowmelt in May. Due to the main snowmelt event most soil infiltration - and consequently also runoff - occurs in this period. The highest values vary from about 18 mm to about 23 mm per day for the studied time period.

2.3.2. *Runoff*

The runoff data for the 50 ha Svartberget catchment was continuously collected at a 90° V-notch weir in a heated house at the outlet of the catchment (Nyberg, 2001). For the simulation, daily average runoff values have been used. Due to sparse snowfall in the year 1996 (Nyberg, 2001) the maximum observed spring runoff peak was only about 5mm. In the two consecutive years 1997 and 1998 more snowfall occurred and therefore higher maximum spring runoff peaks of about 13mm were measured (see Figure 3).

2.3.3. Groundwater level

Groundwater levels for the studied time period were manually measured in perforated groundwater tubes along the transect at the locations S4 to S64. Maximum and minimum groundwater table depths for the studied time period are given in Table 1.

Table 1: Maximum and minimum groundwater table depths from manual observations along the transect between 1996 to 1998

Location	Groundwater table depth (cm)	
	Minimum	Maximum
S4	12.3	103.2
S12	18.5	89.0
S22	40.5	89.5
S40	48.0	96.0
S64	85.3	113.0

It was found that higher groundwater table depths were measured in the months June to August and lower groundwater table depths in the months September to November.

2.3.3.1. Groundwater level – runoff relationship

The relationship between stream-runoff and groundwater table depth in the adjacent hillslope can be used to derive either the discharge from observed groundwater levels, or expected groundwater levels from observed discharge. Depending on local topographic conditions and soil properties, this relationship is different for different locations. Seibert (2003) tested this assumption on two opposing hillslopes located in the Svartberget catchment. He found out that locations closer to the stream show a better correlation of groundwater level and runoff than more distant locations.

Observed discharge data and observed groundwater levels are plotted against each other and different relationships can be fitted. The relationship where the error is least can be seen as representative. To describe transmissivity feedback hypothesis, Bishop (1991) fitted both multiplicative and exponential relationship to data from transects in the Svartberget catchment and Nyberg et al (2001) and Stähli et al (2001) used a logarithmic relationship for the S-transect in Västrabäcken. In this work the same logarithmic relationship was fitted to manual groundwater level observations from 1995 to 1998 (Figure 4). Later on it is used to compare observed and predicted groundwater levels by MIPS.

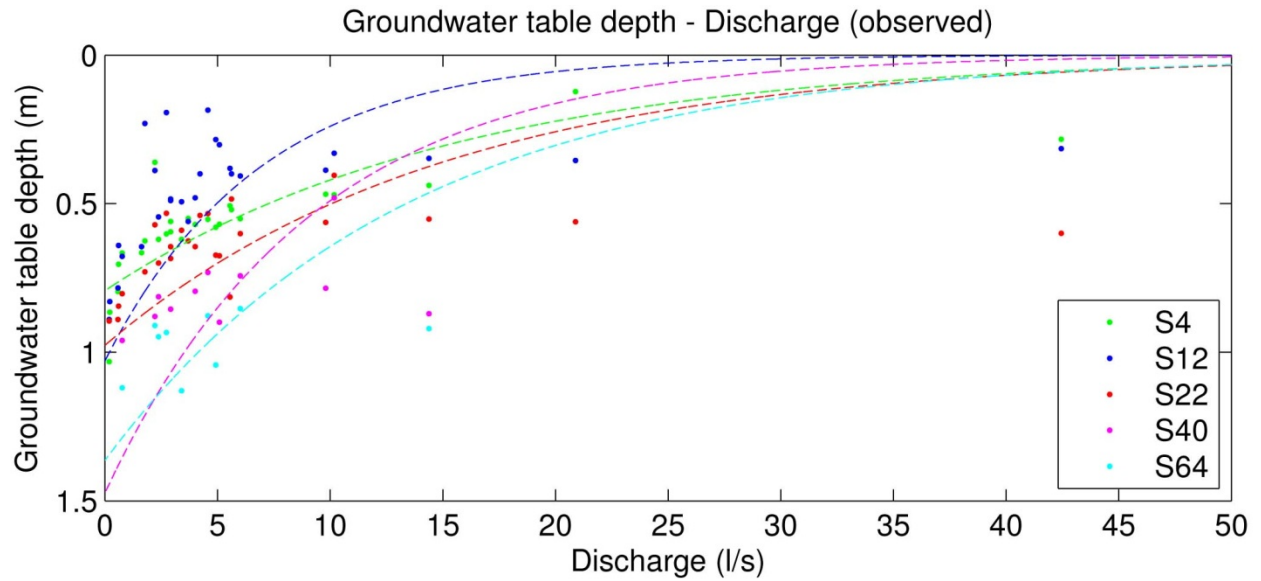


Figure 4: Groundwater table depth – Discharge relationship at different locations along the S-transect. The lines represent the logarithmic relationship

2.3.4. Evapotranspiration

The water losses due to evapotranspiration were found to play a significant role in the water balance of the catchment and evapotranspiration was therefore included in this application of the MIPS model. Since there was no observed data of actual Evapotranspiration estimates for the studied time period available, the widely used HBV model was used to calculate the necessary data using the local water balance (Figure 5).

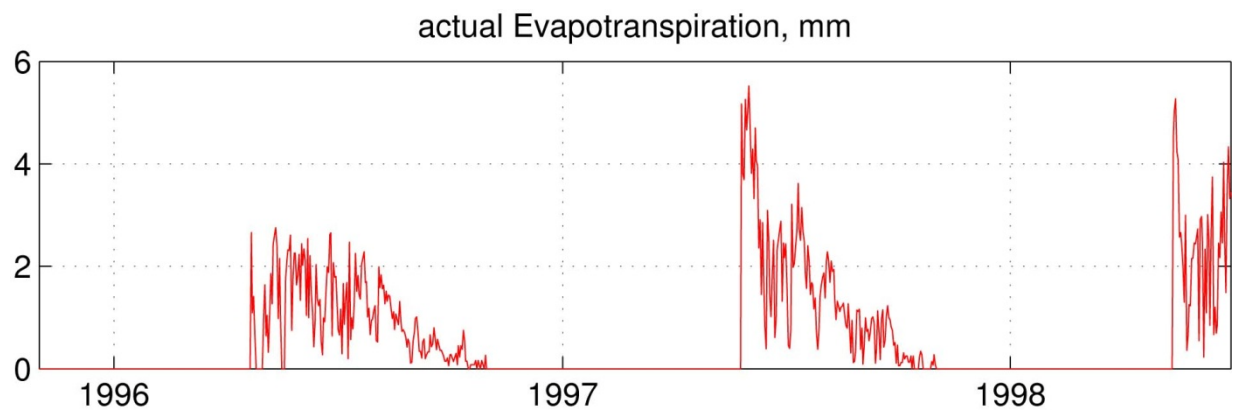


Figure 5: Actual evapotranspiration estimates from the HBV model during the investigated time period

The snow cover in the studied region usually lasts from the beginning of November to the beginning of May. Within this time period the effects of evapotranspiration are at minimum and are therefore not considered. In the middle of June maximum values of more than 5mm per day have been reached in the years 1997 and 1998.

Another parameter influencing the amount of evapotranspiration is the rooting depth which is the soil depth from which water can be taken up by plant roots. A rooting depth of 0.3 m was chosen as reasonable value for the study site location.

2.3.5. Soil properties

Soil properties like saturated hydraulic conductivity and its correlation with porosity are important for the way water moves in soil and have to be well described. Figure 6 shows the different soils and minimum and maximum groundwater levels along the S-transect.

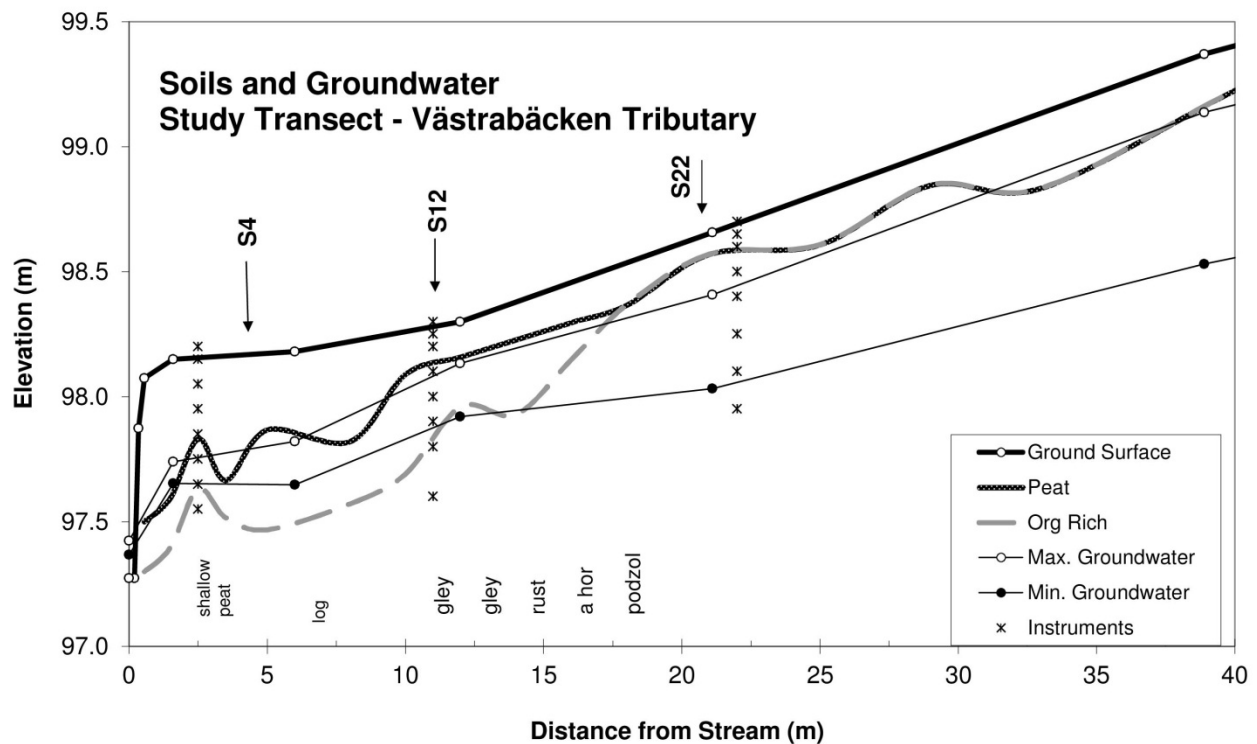


Figure 6: The S-Transect with soil type information, minimum and maximum measured groundwater levels from manual observations and instrumentation (Lysimeter, Piezometer, TDR, Temperature probes, Soil gas probes, Groundwater tubes) locations (from Bishop, 1993)

It can be seen that at the S-transect different kinds of soil are present. Starting from Västrabäcken brook an organic rich soil about 1 m deep and 15 m wide developed where the 0.7 m deep top part is riparian peat soil. After a length of 15 m the organic rich soil gives space to a well drained sandy podzol which is covered with a 20 cm humus layer (Stähli, 2001).

The saturated hydraulic conductivity K_s was estimated from small soil samples using undisturbed soil cores and are only rough estimates of the true values. An exponential relationship between soil depth and K_s was fitted to directly compare the estimates. In Figure

7a it can be seen that the experimentally determined saturated hydraulic conductivity estimates for location S22 are about 10 times higher than for the less conductive peat soil locations S12 and S4. Due to the dense root system in the uppermost horizons this area could not be sampled (Nyberg, 2001). The lack of information about the top part of the soil may have some influence on testing the transmissivity feedback hypothesis at that site.

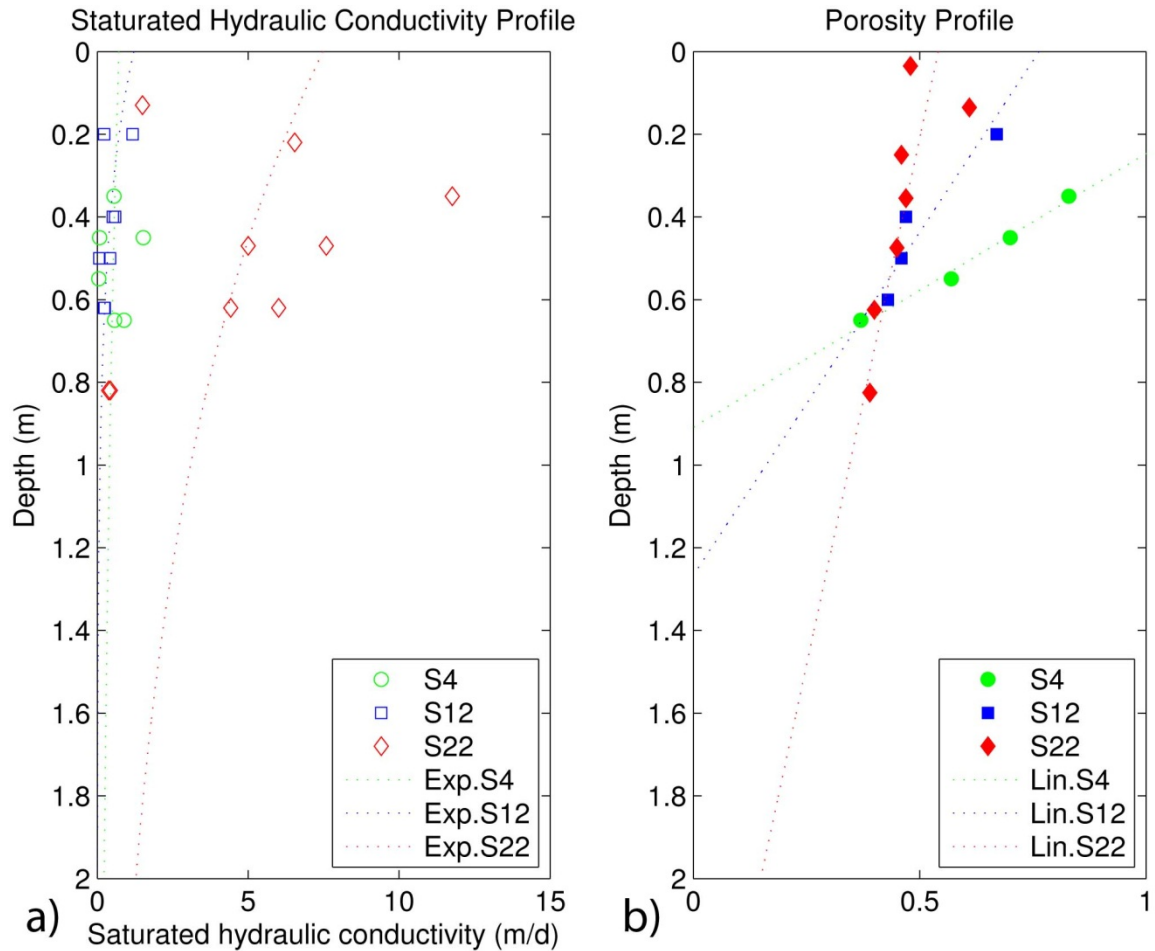


Figure 7: a) Saturated hydraulic conductivity profile and exponential regression relationship for location S4, S12 and S22; b) Porosity profile and linear regression relationship for location S4, S12 and S22 (after Nyberg, 2001)

Soil porosity is important for estimating water storage abilities of a soil and consequently also groundwater levels. For the S-transect the estimated soil porosities vary considerably for the different locations due to the shift from peat to mineral soil. In Figure 7b it can be seen that the decrease in porosity with depth is way higher for the peat soil close to the stream (S4 and S12) than for the more distant podzol soils (S22 and further away). The linear regression relationship was added to compare and point out the differences among the studied locations.

In this work porosity estimates from samples have been found to be quite reasonable and are therefore well suited for comparisons with the used MIPS input parameters. Values for the

saturated hydraulic conductivity have not been found to reflect the real soil properties as accurate.

2.4. Model description

As the name MIPS (Multiple Interacting Pathways) of the model already reveals it's dealing with possible groundwater flow pathways within a slope. By treating water as particles with a certain volume and velocity and given limitations from the soil the particles can be followed throughout their journey through the slope.

The basic idea behind the concept is to account soil heterogeneities by using transition probability matrices which 'describe the probability of a particle entering a certain pathway, conditional to its current pathway' (Davies et al., 2011). In terms of particles it can be seen as the probability that one particle changes from one pathway to another. From an initial start on the particle moves within its potential flow pathways according to step equations which are used to move the particle from one position to another.

The velocity is assigned randomly according to a certain velocity distribution. Depending on the soil type and especially heterogeneities like the amount of macro pores, worm holes or cracks which may be seen as preferential flow pathways these velocity distributions will differ for different locations. Since the particles are identifiable fluid material volumes that are carried about with the flow the assigned velocities are Lagrangian velocities (Price, 2006). For simplification purposes there is no exchange between two crossing particles considered.

In this work transition probability matrices have also been used to simulate the effect of evapotranspiration. This was done by first identifying particles which are available for evapotranspiration depending on the root depth and second by picking randomly from those available particles. Another application for transition probability matrices can be simulation of deep drainage loss. By accounting for the unevenness of soils by velocity distributions and transition probability matrices the effects of preferential flow pathways can be taken into account without knowing the geometry and spatial distribution of those (Davies, 2011).

In the MIPS model soil properties are not only derived from small soil samples which can only be representative for a small area they are taken from but not for whole slopes, soil bodies or even catchments. Model parameters, like the surface saturated soil conductivity, are not derived from soil samples but by selecting those model responses which fit best to observed response data. The combination of parameters used for a run where the error of observed and predicted data is least can be seen as representative for the studied hill slope.

The aim behind this idea is not to minimize the amount of parameters or calibration efforts but to encourage hydrologic modelers to reconsider the complexities of soil-water interactions especially for hillslopes.

2.4.1. Slope set-up

The S-transect is located in the catchment of Västtrabäcken and was chosen as a test site for this work. The application of MIPS here is only two dimensional (2D). A three dimensional (3D) application would also be possible but would be more time and data demanding. For a clear understanding of the following model component explanations Figure 8 illustrates the considered slope geometries and basic model assumptions.

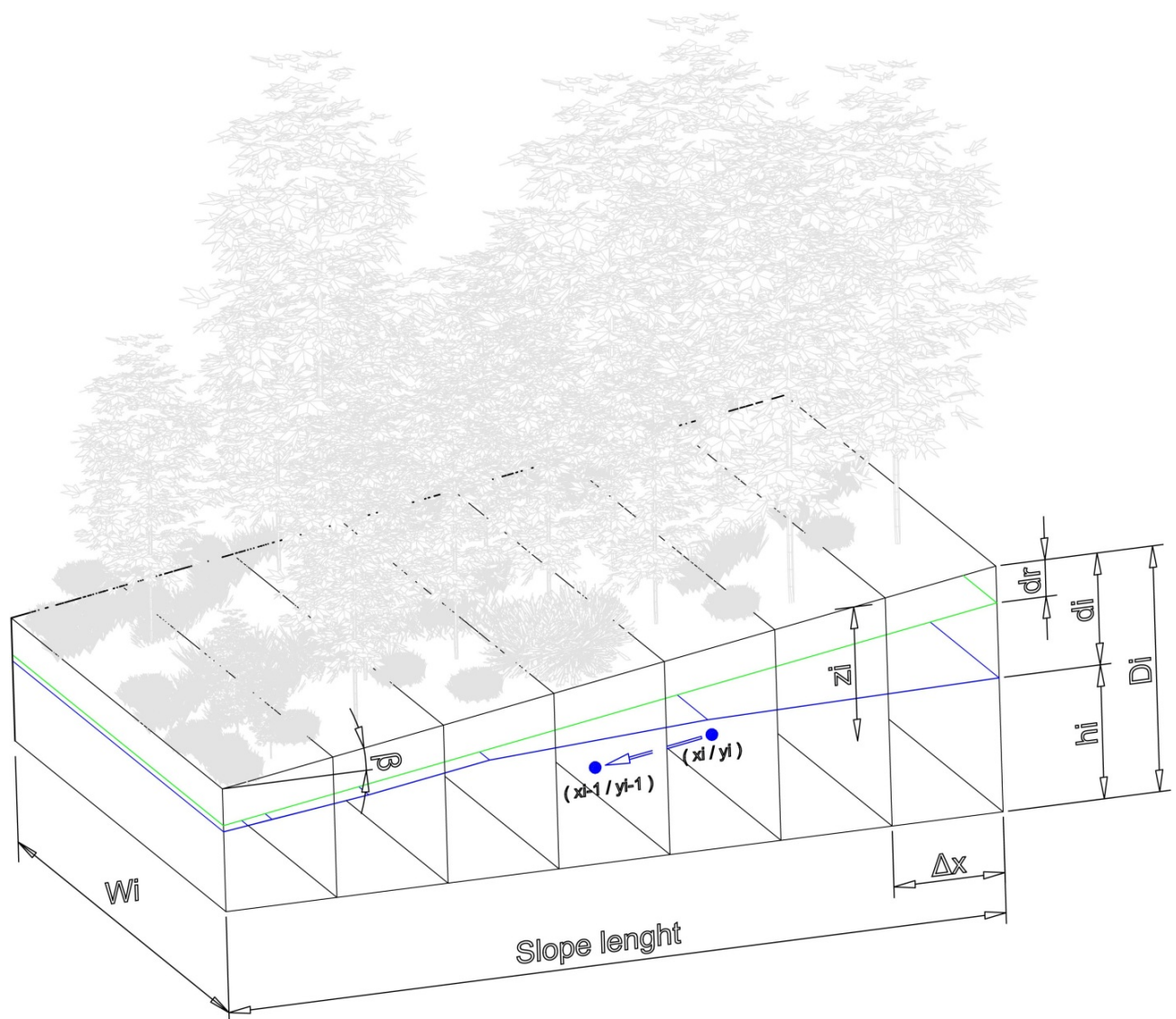


Figure 8: Slope geometries and basic model assumptions

Throughout a length of 64 m the slope reaches from the stream (Västrabäcken) to the watershed divide of the catchment. The chosen simulation width is 10 m. Since the top end of the slope reaches the catchment boundary there is no upslope input into the slope and lateral input from both side walls of the slope are negligible and therefore not considered in the simulation. The gradient of the surface slope is approximated to be constant over the whole length.

The assumed slope depth varies between 1 m at the lower and 2 m at the upper boundary of the slope. Even though bedrock isn't reached before 5-6 m depth (Nyberg, 2001) lower soil depths (1-2 m) are found reasonable for the simulation because of declining saturated hydraulic conductivities at greater depths.

According to the 'transmissivity feedback hypothesis' which says that the transmissivity of a soil increases rapidly with rising groundwater table (Bishop, 1991) the relationship of saturated hydraulic conductivity at any depth K_s (m/day) and soil depth below the surface z (m) can be defined as:

$$K_s = K_0 \exp(-fz) \quad (1)$$

where K_0 is the hydraulic conductivity at surface level and f is a parameter.

The estimates of measured K_s are derived from small undisturbed soil cores and are shown in Figure 7a. These estimated values are only poor estimates of the true K_s of a till soil and are generally underestimated (Bishop, 1991). Therefore Stähli (2001) used calibrated K_s values (see Figure 9a) to test the physically based COUP model at the S-transect.

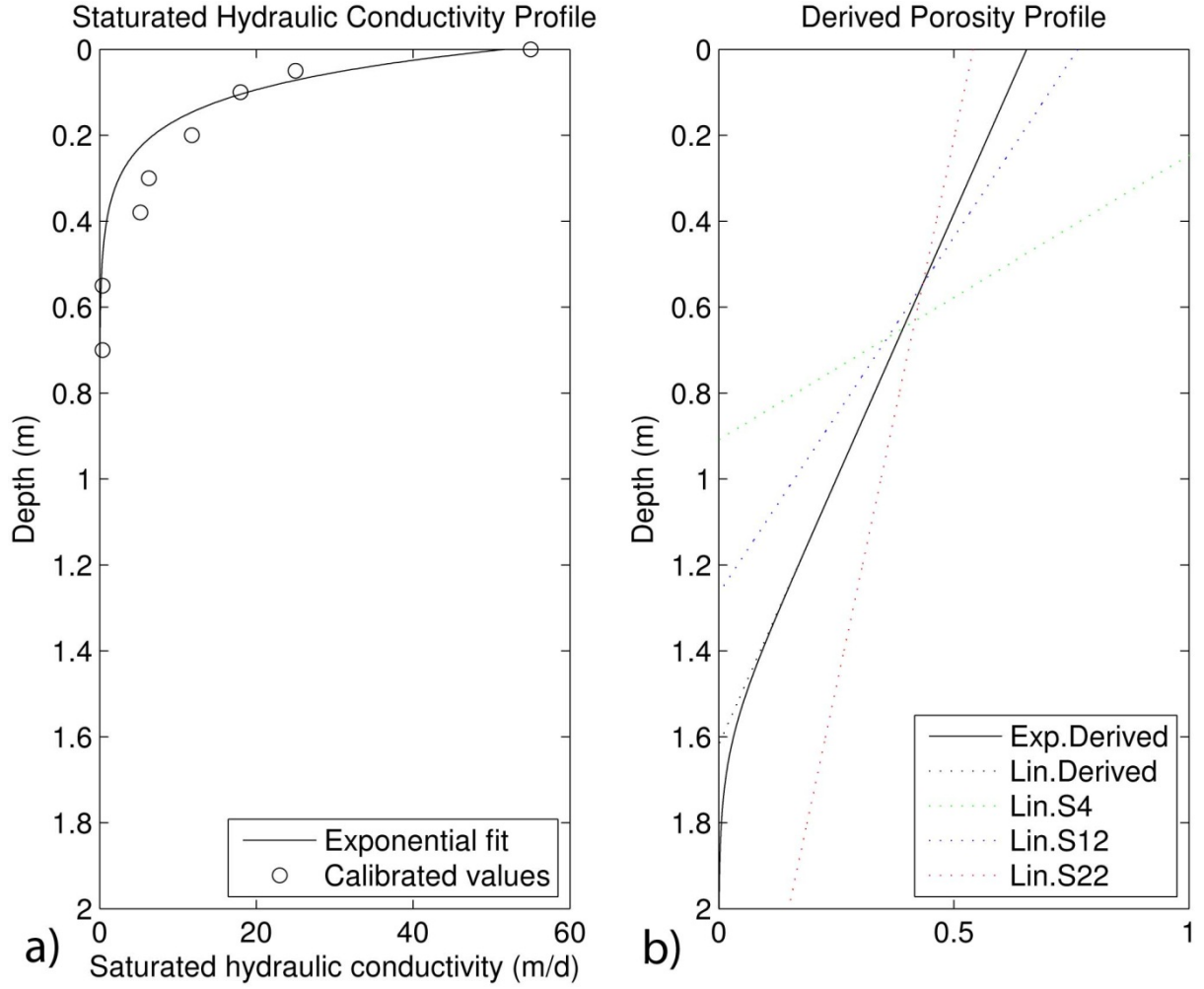


Figure 9: a) Assumed saturated hydraulic conductivity profile (after Stähli, 2001) with exponential regression relationship; b) Derived porosity profile with parameters: $K_0 = 52$ m/day; $f = -10$; $v_0 = 0.0001$ m/day and $b = 25$ and linear relationship from soil samples for location S4, S12 and S22

Since the problem of imprecise sample estimates and the occurrence of different soil types is still valid these calibrated K_s values have been selected as a useful starting point for the MIPS simulation. The exponential relationship of the assumed hydraulic conductivity profile with depth is depicted in Figure 9a.

The local transmissivity T_i characterizes the amount of water obtainable under a unit hydraulic gradient (Hillel, 2004). It can be derived by integrating K_s from the local soil depth D to the depth of the water table d .

$$T_i = \int_d^D K_0 \exp(-fz) = \frac{K_0}{f} [\exp(-fd) - \exp(-fD)] \quad (2)$$

The velocity of each particle at any depth z is then randomly assigned depending on the exponential relationship:

$$v = v_0 \exp(b\theta) \quad (3)$$

where θ is the pore space filled with mobile water, v_0 is the assumed minimum mobile velocity and b is the parameter that determines the exponential increase of velocity with porosity (Davies, 2011). The saturated hydraulic conductivity at any depth K_s can then be recalculated by integrating v from 0 to the saturated porosity θ_s .

$$K_s = \int_0^{\theta_s} v \, d\theta = \frac{v_0}{b} [\exp(b\theta_s) - 1] = K_0 \exp(-fz) \quad (4)$$

Based on those formulations the change in porosity θ_s with increasing depth z can be derived as:

$$\theta_s = \frac{\ln \{1 + K_0 b \exp(-fz)/v_0\}}{b} \quad (5)$$

The estimated porosity profile shows an assumed linear decrease of porosity with depth (Figure 9b) which corresponds well to the loss of macro pores with depth.

Some important findings considering the structure of the model can be identified. The porosity profile is derived from the conductivity profile and the velocity distribution. If measured porosity data is available it can be used to check chosen parameters values by comparing it with derived porosity data. Furthermore the shape and form of both the conductivity and velocity distribution may vary for different soils what has to be considered when applying the model to different sites.

2.4.2. Defining initial conditions

Initial conditions need to be identified in order to obtain reasonable outputs from an early computing stage on. In MIPS, the first thing to do is to fill up the soil with particles according to the pre-defined soil properties especially the porosity profile. Given the assumption that at initial time the slope is at steady state the discharge in the stream can be used as a rough estimate of the recharge rate from the unsaturated zone.

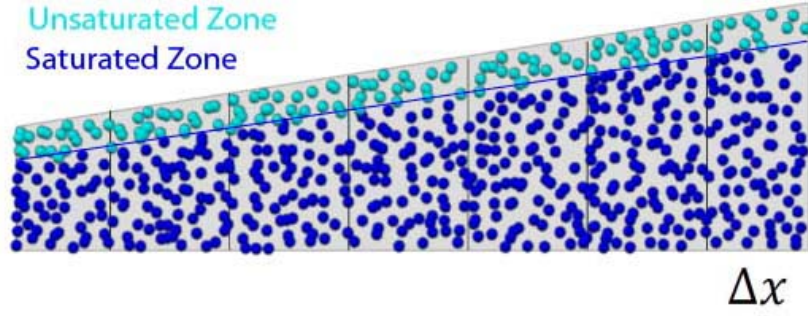


Figure 10: Slope profile showing step size, unsaturated and saturated zone

Using these two assumptions, saturation can be calculated along the slope using a certain slope length step size (see Figure 10). The way the step size is chosen has a strong influence on the resolution of saturation representation and computing time. In general it can be said that the shorter the step size the better the resolution and the longer the computing time. In this work a step size $\Delta x = 1$ m was chosen.

Saturation at top of the slope is dependent on the initial upslope flux per unit width q_u (m²/day), the initial lateral flux per unit length along the slope q_l (m²/day) and the initial recharge from the unsaturated zone per unit area r_0 (m/day) (see Figure 11).

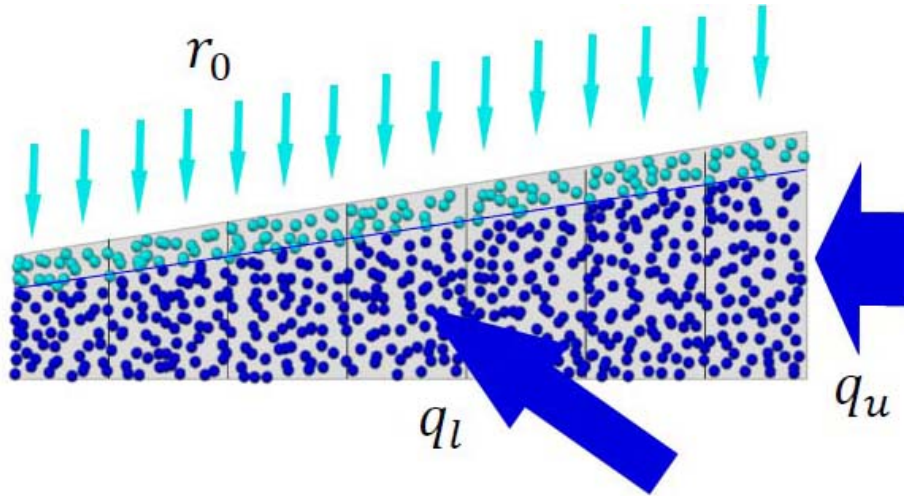


Figure 11: Slope profile with recharge from the unsaturated zone, initial upslope- and lateral flux

Adding up those three inputs gives an expression for the volumetric flow rate across the slope Q_i (Davies et al, 2011):

$$Q_i = Q_{i-1} + \Delta x q_l + \Delta x W_i r_0 \quad (6)$$

where Δx is the slope length step size and W_i (m) is the slope width at step i . Then the volumetric flow rate of the first increment Q_1 is:

$$Q_1 = W_0 q_u + \Delta x q_l + \Delta x W_1 r_0 \quad (7)$$

where W_0 (m) is the slope width at the upslope boundary of the first increment and W_1 is the slope width at the downslope boundary of the first increment.

Since upslope and lateral inputs are not relevant for the S-transect slope only recharge from the unsaturated zone has to be included. This may be different for different sites where upslope and lateral input plays a more or less important role depending on the catchment shape and position of the slope within the catchment.

The hydraulic gradient is assumed to be constant over the whole slope length and is equal to the surface slope which is a function of the surface slope angle β . Assuming a constant hydraulic gradient and hydraulic conductivity profile the specific discharge q is:

$$q = K_0 \exp(-f(D - h)) \sin \beta \quad (8)$$

with h (m) as the height of the water table from the slope bottom. The water table depth profile along the slope length can then be derived by integrating this downslope discharge within the water table and relating this to the volumetric flow rate across the slope:

$$d_i = -\frac{1}{f} \ln \left(\exp(-fD_i) - \frac{f}{K_0 \sin \beta} Q_i \right) \quad (9)$$

Knowing the local water table depth d_i (m) and soil depth D (m) the local water storage in the saturated zone S_i (m³/m) is calculated by integrating the porosity function from the bottom of the slope to the water table depth (see Figure 12):

$$S_i = \frac{1}{2} (D_i - d_i) W_i \left(\frac{1}{b} \ln \left(1 + \frac{K_0 b}{v_0} \exp(-fD_i) \right) + \frac{1}{b} \ln \left(1 + \frac{K_0 b}{v_0} \exp(-fd_i) \right) \right) \quad (10)$$

This storage volume can always be converted to the number of particles required depending on the previous defined volume of a single particle.

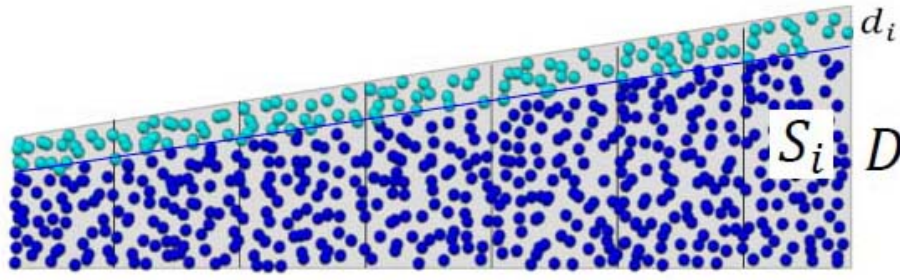


Figure 12: Slope profile with water table depth, soil depth and water storage in the saturated zone

The chosen volume of a particle also determines the accuracy of the representation of the water storage (Davies, 2011). The lower the volume is the better the accuracy and the higher the computational requirements. In this work the particle volume is 1 liter. This value was found to be sufficient in terms of accuracy and to keep computation times reasonable.

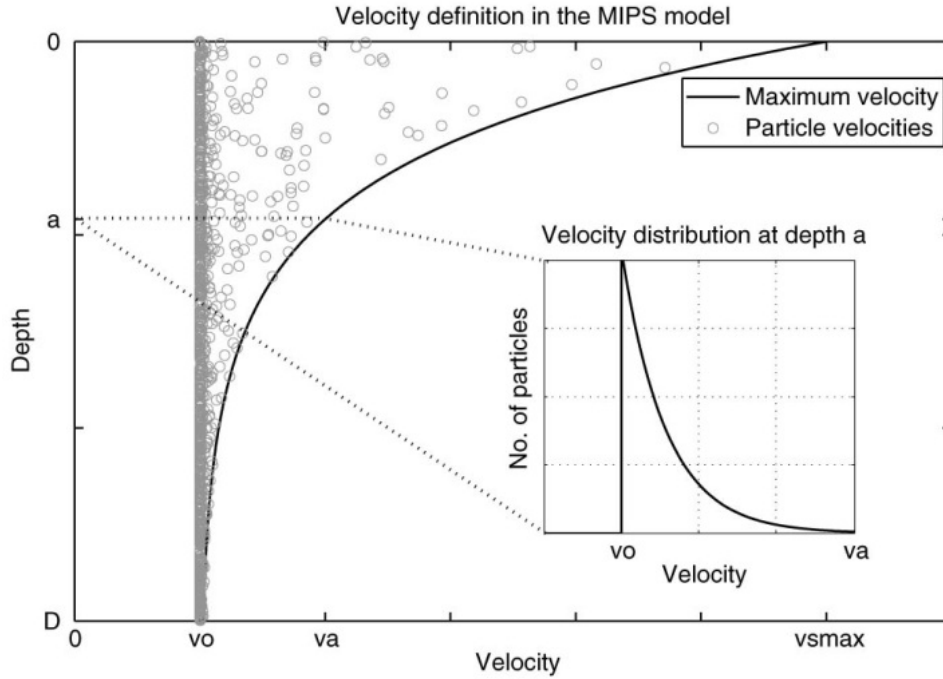


Figure 13: Representation of how velocities are assigned according to an exponential distribution between a minimum and maximum velocity and Equation 3 (from Davies, 2011)

In the initial state vertical and lateral positions within the saturated zone of the slope are assigned randomly to each particle. Depending on its position and using Equation 3 a particle velocity is assigned randomly. Figure 13 illustrates how velocities are assigned for particles at a certain depth a . The exponential relationship reveals that most particles are moving at slow velocities and for accounting preferential flow pathways only a few are having high velocities assigned.

In the unsaturated zone particles are only moving vertically under a unit hydraulic gradient. Therefore the volume of water within this zone is only dependent on the initial steady recharge rate:

$$\theta = \frac{1}{b} \ln \left(1 + \frac{r_0 b}{v_0} \right) \quad (11)$$

The volumetric soil wetness θ can then be transformed to number of particles required in the previously explained way.

The particles representing the initial storage in both unsaturated and saturated zones prior to an event can be labeled as “old” or “pre-event” particles (Davies, 2011).

2.4.3. Defining the input boundary conditions

Depending on the slopes position within the catchment some assumptions concerning the way in which water is distributed and enters the slope have to be made. Simplified assumptions to start with are that surface inputs like precipitation are distributed evenly along the slope. The time when a particle enters the slope can be stored and used for residence time analysis. A simpler way is to distinguish between “pre-event” and “event” particles. As soon as a particle enters the slope a velocity is assigned according to the way described in the previous chapter.

Furthermore inputs originating from the upslope and surrounding catchment can be integrated into MIPS using a simple time-invariant linear store. These upslope and lateral input regions can be represented as two stores in parallel, with different time constants that feed into the upper and lateral boundaries of the slope (Davies, 2011). Davies (2011) applied MIPS to a tracer experimental plot in Gårdjön using upslope and lateral input stores. There the flanking regions were considered as responding quickly with a shorter time constant and the convergent central valley region had a slower response with a longer time constant.

Given the local topography of the S-transect position within the catchment the following assumptions concerning its boundary conditions have been made. The upper slope boundary is also the catchment boundary and therefore no upslope input occurs. Laterally, the slope is approximately bounded by streamlines, so that no lateral input from both flanking regions occurs. Applying MIPS to a slope where no upslope and lateral inputs need to be considered decreases the amount of required parameters and the errors resulting from calibrated time constants.

2.4.4. Defining the step equations

From an initial starting time onwards, particles inside the slope are moving differently depending whether they are situated in the unsaturated or saturated zone. Particles within the saturated zone are moving parallel to the constant surface slope which is also equal to the hydraulic gradient (see Figure 14). Following a particle from one position to another the horizontal change in space is:

$$x_i = x_{i-1} + \tan(\beta) v t_s \quad (12)$$

where t_s is the time step, x is the horizontal position of the particle within the saturated zone and v is the randomly assigned velocity according to the unit hydraulic gradient. In cases where the slope depth and width changes along the slope mass balance is maintained by changing the particles vertical position proportional to the change in depth of saturation (Davies, 2011). Since the slope width is equal for the whole slope length only changes in depth need to be considered in this work.

Particles situated in the unsaturated zone are assumed to only move vertically (see Figure 14). The vertical change in space is defined as:

$$y_i = y_{i-1} + v t_s \quad (13)$$

where y is the vertical position of the particle within the unsaturated zone.

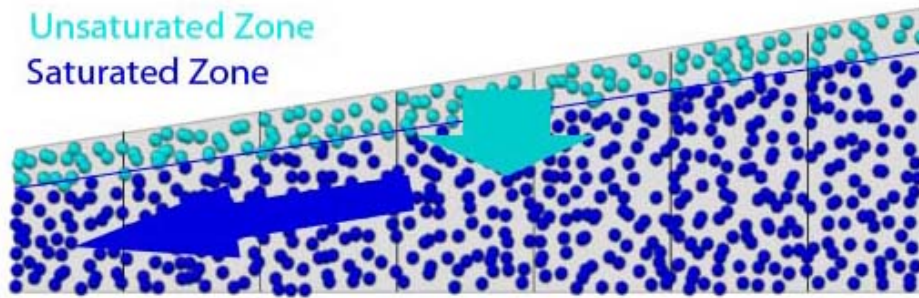


Figure 14: Slope profile with schematic particle movement

After moving the particles in the slope as described above and adding upslope and lateral inputs to the slope, the new water table depth is recalculated following steps described below:

1. Calculating the expected local volume of water below the water table V (m^3) for a unit length increment Δx by counting the number of laterally moving particles.

2. Assuming the porosity decrease with depth as linear (see Figure 9b) and that all laterally moving particles are below the water table in the saturated zone, the expected volume is:

$$V = 0.5(\theta_d + \theta_D)(D - d)W\Delta x \quad (14)$$

and the porosity at water table depth θ_d is:

$$\theta_d = \theta_0 + \frac{(\theta_D - \theta_0)}{D}d \quad (15)$$

where θ_D is the porosity at the bottom and θ_0 is the porosity at the surface of the increment. Combining Equation 14 and 15 gives a quadratic equation where the new water table depth can be derived from:

$$\frac{(\theta_D - \theta_0)}{D}d^2 + 2\theta_0d + \frac{2V}{W\Delta x} - D(\theta_D + \theta_0) = 0 \quad (16)$$

3. Depending on the particle's position relative to the new calculated ground water table it is relabeled. For example will a particle which moved into the unsaturated zone but now lies below the ground water table will be labeled as saturated whereas a particle which is above the ground water table will be labeled as unsaturated.
4. If overland flow occurs, which is a result of over-saturation of soil, porosity above the surface is assumed to be unity (Davies, 2011).

Different than for subsurface flow, overland flow particle velocities are assigned using a uniform rather than an exponential distribution. By using a uniform velocity distribution and additionally a multiplier in order to achieve average velocities the error between predictions and observations becomes less and therefore more realistic simulation results can be achieved. Here it should also be stated that once a particle is labeled as overland flow it can't infiltrate into the soil anymore.

2.4.5. Defining the transition probability matrices

As stated earlier the transition probability matrix expresses the probability for a particle to change from its current pathway to another depending on the current pathway's conditions. For example, the probability for a particle to enter a slow pathway from a fast pathway will be different than for a particle entering a fast pathway from a slow pathway. These transition

probabilities are strongly dependent on capillary effects, evaporative demand and local interactions between macropores and matrix (Davies, 2011).

In this work the simplest possible case was chosen which means that all transition probabilities except for evapotranspiration are set to zero. By doing so once the particle enters the saturated zone and has a velocity assigned, it travels at the same velocity until it reaches the lower boundary of the slope or exfiltrates onto the surface (Davies, 2011). This means that the term of Lagrangian velocity is defined here as the current velocity of the particle in its current pathway.

2.4.6. Defining evapotranspiration

Depending on the site's location, evapotranspiration has a significant influence on the water balance over a whole hydrologic year. Adding evapotranspiration to the system may reduce the recharge from the unsaturated zone and lower the water tables. Furthermore it will influence the variation of discharge rates with current slope conditions depending on the exponential saturated conductivity profile.

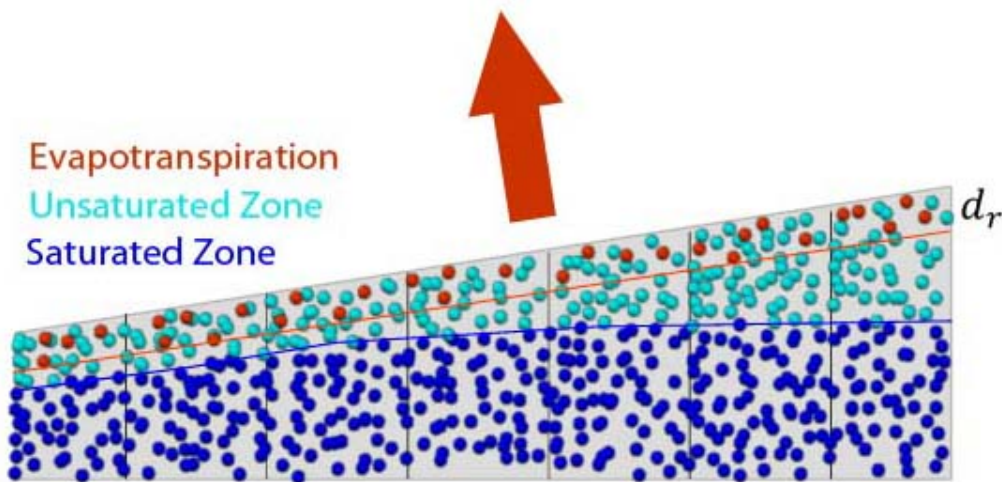


Figure 15: Slope profile with evapotranspired particles, particles in the unsaturated and saturated zone

In terms of evapotranspiration the transition probability matrix can be implemented in the following way:

1. Calculating the number of particles which need to be evapotranspired according to calculated daily actual evapotranspiration estimates. If there is no calculated data available potential evapotranspiration data can be used as rough estimates and a seasonal sine curve can be used for determining missing estimates.

2. Calculating the availability of particles in the slope for evapotranspiration depending on its rooting depth (see Figure 15). This can be done by assuming a linear decrease in availability of 100% at the surface to 0% at rooting depth level which is given in Equation 17:

$$Av = ay_i + b \quad (17)$$

where Av is the particle's availability at any depth y_i , b is the availability at surface level and $a = b/d_r$ is a factor for linear decrease where d_r is the rooting depth.

3. If there are enough particles available in the slope depending on its current conditions particles are randomly chosen from this set and labeled as 'evapotranspired' until the required amount of particles to be evapotranspired (Step 1) is met. If there are fewer particles available than required all available particles are chosen and labeled as 'evapotranspired'.
4. To complete the process evapotranspired particles are labeled as 'exited' and moved outside the slope. At this stage the time of exit and number of particles exited as evapotranspiration can be stored for later analysis.

2.5. Model settings

The way input parameters are chosen has a strong influence on the output quality of the MIPS model. Since not all parameters are calibrated but more derived from soil properties (particularly saturated hydraulic conductivity and porosity) the main focus is on these. A summary of the chosen parameters for the initial run is given in Table 2.

Table 2: Parameters required by the MIPS model (Run(52/10))

Parameter	Units	Initial values
Slope length	m	64.00
Slope width	m	10.00
Soil depth	m	1.0 - 2.0
Slope angle	deg	1.72
Downslope length increment	m	1.00
Time increment	h	2.00
Particle volume	l	1.00
Saturated hydraulic conductivity at soil surface	m/d	52.00
Exponential parameter for decline of hydraulic conductivity with	m ⁻¹	-10.00
Exponential parameter for the increase of velocity with saturation, b	-	25.00
Minimum mobile velocity, v_0	m/d	0.0001

Estimates of the saturated hydraulic conductivity are derived from small soil samples by Nyberg (2001). Since these estimates are only an approximate representation of the real values and are usually underestimated (Bishop, 1991) more realistic values have been calibrated by Stähli (2001) from the relationship between groundwater level changes and runoff. Using an exponential regression relationship a continuous conductivity profile was derived giving the values for the initial run of the model which was named Run(52/10) where 52 is the value for K_0 and 10 is the f-value.

Another indicator that these first parameter estimates are a good starting point is the good correlation of the derived and measured porosity profile. Comparing Figure 7b and Figure 9b it can be seen that the derived porosity profile is similar to the one of location S22 which was found as most representative for the whole slope.

The slope geometry was approximated using information from earlier research conducted at the S-transect by Bishop (1993). The slope has a length of 64 m and extends from the stream Västrabäcken to the catchment boundary. The lateral groundwater movement is parallel to the oblique angle of the transect to the stream which means that no lateral and upslope input occurs to the system.

The parameters increment length, time increment and particle volume are mainly influencing the resolution of the model outputs. By decreasing their values a higher resolution can be achieved which consequently leads to increasing computation durations. In this work those parameters have been set to values which seemed reasonable in terms of output resolution and computation duration.

In order to answer the questions stated in the introduction, a set of surface saturated hydraulic conductivity K_0 and decreasing factor f was chosen to which MIPS was applied. Figure 16 gives an overview of those parameter sets.

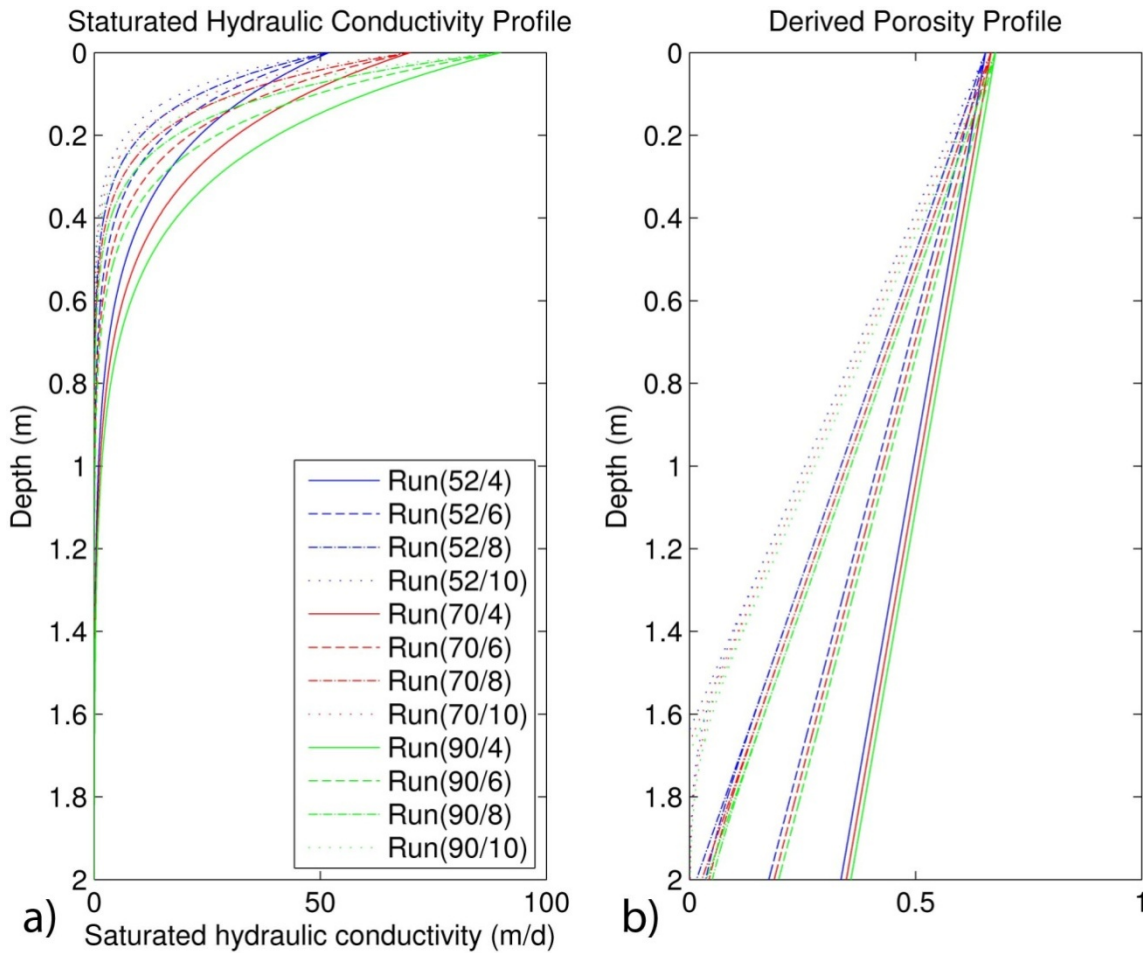


Figure 16: Set of K_0 and f combinations used for running the MIPS model

Additional runs were made for different time periods. The above mentioned model runs (Figure 16) were conducted for both a whole hydrological year (01.10.1996 – 30.09.1997) and a longer time period (01.11.1995 – 30.06.1998). This may reveal long term effects on the hydrograph and groundwater level as well as to examine the assumption that at initial time the slope is at steady state conditions.

2.6. Parameter sensitivity analysis

To examine the performance of rainfall-runoff models some measures can be applied. As mentioned in the introduction the purpose for applying rainfall-runoff models, beside others, is to predict hydrograph peaks and the timing of the hydrograph peaks correctly (Beven, 2012).

In hydrograph simulation one measure for the goodness – of – fit of predicted and observed discharge is to take the sum of squared errors or the error variance σ_ε^2 . This can be done by squaring the difference between predicted discharge \hat{y}_t and observed discharge y_t , summing up the values for every time step $t = 1, 2, \dots, T$ over the whole simulation period and divide the sum by the amount of time steps T .

$$\sigma_\varepsilon^2 = \frac{1}{T-1} \sum_{t=1}^T (\hat{y}_t - y_t)^2 \quad (18)$$

Another widely used measure is the simulation “efficiency” of Nash and Sutcliffe (1970):

$$E = \left[1 - \frac{\sigma_\varepsilon^2}{\sigma_o^2} \right] \quad (19)$$

where σ_o^2 is the variance of the observed discharge. The value of efficiency for a perfect fit of predicted and observed data is 1 when σ_ε^2 is 0. An efficiency value of 0 indicates that σ_ε^2 is equal to σ_o^2 which means that the model is no better than a one parameter “no knowledge” model and a negative efficiency value indicates an even worse performance than a “no knowledge” model (Beven, 2012).

3. Results

3.1 Model performance

In this work the error variance and the efficiency after Nash and Sutcliffe (1970) were used as goodness – of – fit measure of the observed and predicted hydrographs. Both measures were applied to simulations covering one hydrological year, so called short period simulations (01.10.1996 – 30.09.1997) and some consecutive years before and after that, so called long period simulations (01.11.1995 – 30.06.1998). The outcomes are summarized in Table 3.

Table 3: Error variance and efficiency after Nash and Sutcliffe (1970) for all conducted short period and long period MIPS simulations

	Soil properties		Error variance σ_{ϵ}^2		Efficiency	
	K_0	f	short	long	short	long
Run(52/4)	52	4	0.75	0.75	0.70	0.66
Run(52/6)	52	6	1.28	1.19	0.48	0.46
Run(52/8)	52	8	2.07	1.79	0.16	0.18
Run(52/10)	52	10	2.56	2.05	-0.04	0.06
Run(70/4)	70	4	0.96		0.61	
Run(70/6)	70	6	0.96	1.04	0.61	0.52
Run(70/8)	70	8	1.77	1.65	0.28	0.24
Run(70/10)	70	10	2.32	1.93	0.06	0.11
Run(90/4)	90	4	1.46		0.41	
Run(90/6)	90	6	0.78		0.68	
Run(90/8)	90	8	1.60		0.35	
Run(90/10)	90	10	2.18		0.11	

Compared to the initial simulation Run(52/10), it can be observed that the error variance decreases with a decreasing parameter f and with increasing surface saturated hydraulic conductivity. Consequently the efficiency increases with decreasing f-value and increasing surface saturated hydraulic conductivity. Furthermore, it was found that the efficiencies change depending on the f-value and simulation period. Comparing short- and long period simulations it can be seen that higher f-values give higher efficiencies and lower f-values give lower efficiencies for long period simulations.

The highest achieved efficiency of all conducted simulations is 0.70 for the short period simulation Run(52/4). The lowest calculated efficiency is -0.04 for the short period initial simulation Run(52/10).

The same procedure of performance determination can be applied to observed and predicted groundwater levels which would be of great interest in terms of geochemical modeling.

3.2 Drainage and stream runoff

One important issue in terms of model understanding is to examine in which way and to what extent the hydrograph changes when certain model parameters change. Figure 17 shows the hydrograph of the initial simulation Run(52/10) in relation to the observed stream runoff, precipitation and actual evapotranspiration. It can be seen that the timing of the simulated hydrograph peaks corresponds well with the timing of the observed precipitation and runoff but the simulated values were often over- or under-predicted.

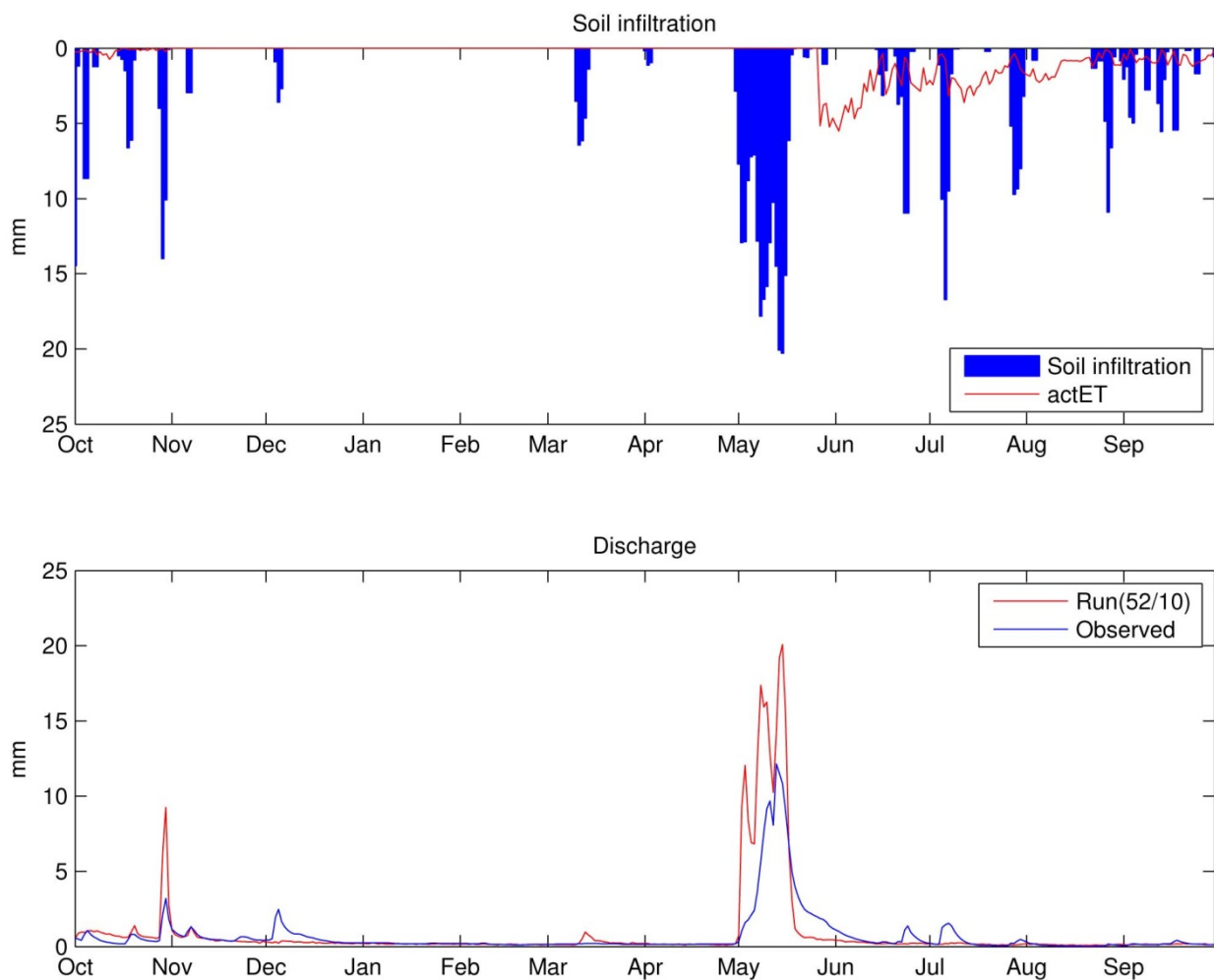


Figure 17: Daily soil infiltration, actual evapotranspiration and predicted versus observed hydrographs for simulation Run(52/10)

Both the simulated peaks and the timing of those peaks may vary according to the chosen parameter combination. Figure 18 shows the hydrographs of all used parameter combinations and observed discharge. One finding is that no simulation could predict the small observed peak at the beginning of December while most simulations over-predicted the peaks of the spring event from May to June. The small peaks at the end of June and beginning of July were generally slightly under-predicted.

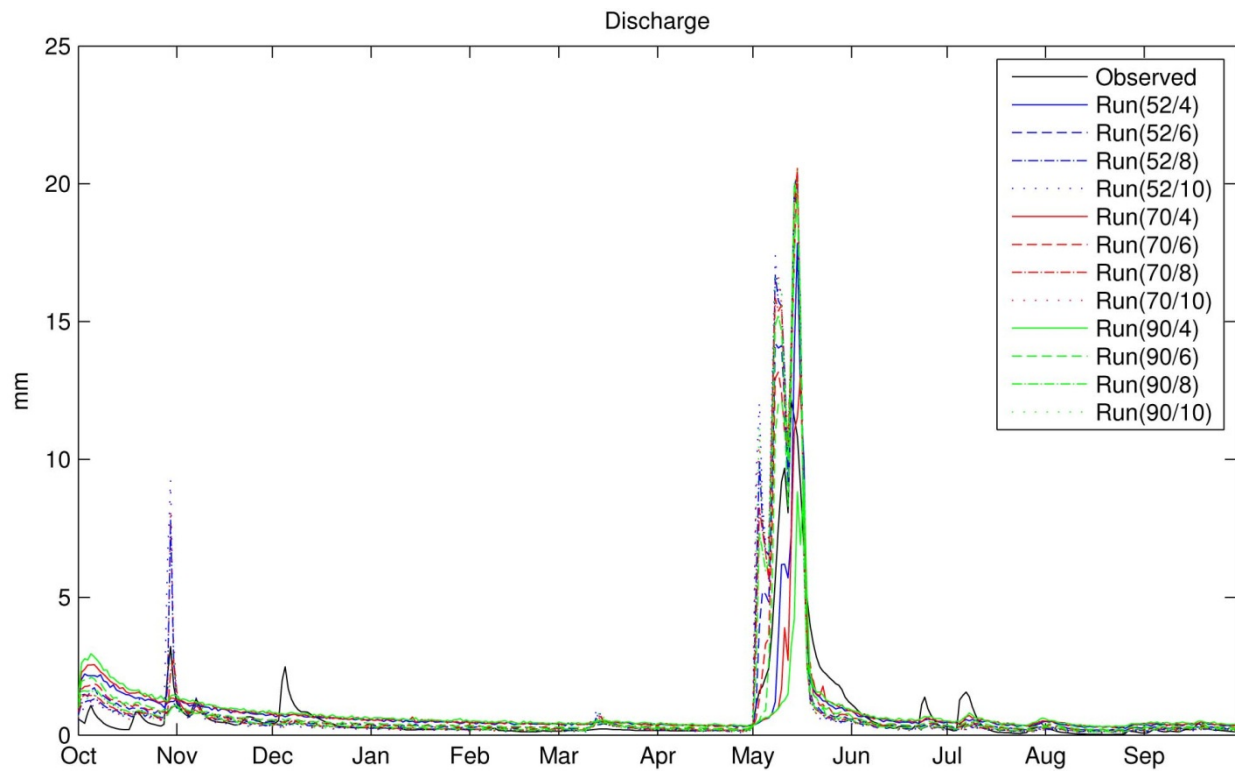


Figure 18: Observed and predicted hydrographs for all considered parameter combinations

3.2.1. The influence of changing the surface saturated hydraulic conductivity

By choosing and comparing simulation runs where the surface hydraulic conductivity changes but the f – value stays constant, the influence of changes in surface saturated hydraulic conductivity can be identified. In Figure 19 it can be seen that high hydrograph peaks are decreasing with increasing surface hydraulic conductivity. The base flow, especially during winter season from January to May, was well reproduced by the model and is almost equal for all parameter combinations.

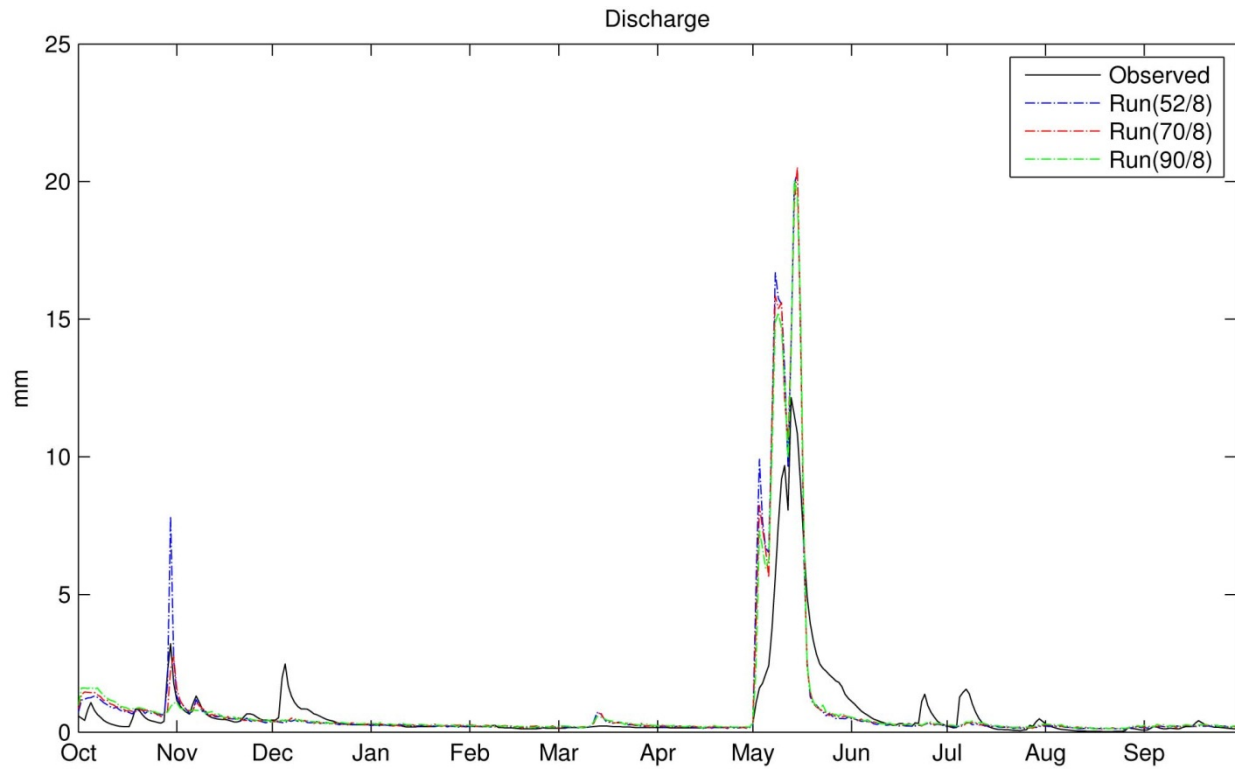


Figure 19: Observed and predicted hydrographs for simulations with changing surface saturated hydraulic conductivity and $f = 8$

3.2.2. The influence of changing the f -value

Beside the surface hydraulic conductivity it is the f -value that is primarily influencing the simulation outputs. By decreasing f the high peaks during autumn and spring are reduced and the base flow increases (see Figure 20). While a low f -value is over-predicting the runoff during winter season, and high f -values are over-predicting the runoff during bigger runoff events in autumn and spring. It was also found that the timing of the peaks is influenced by a changing f -value. A good timing of the spring runoff event was achieved for the f -values 6,8 and 10 while the timing for a f -value of 4 was delayed.

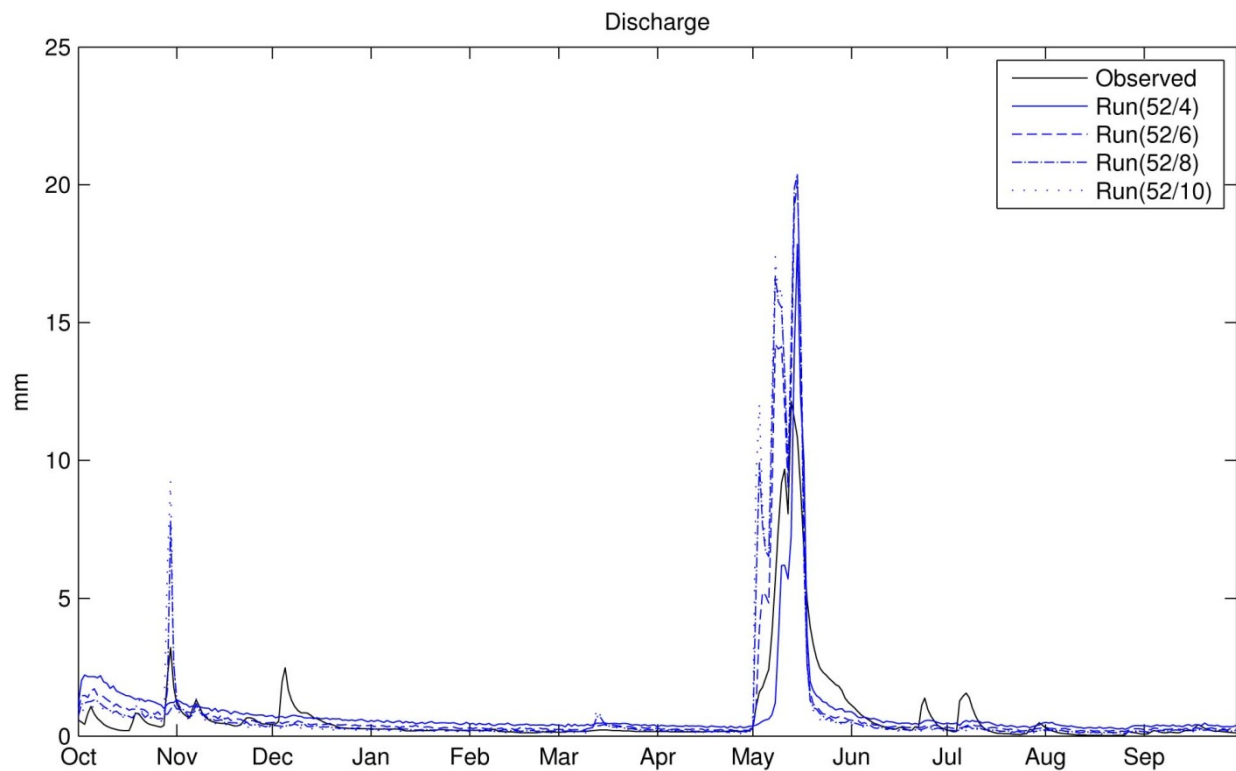


Figure 20: Observed and predicted hydrographs for simulations with changing f -values and $K_0 = 52$

3.2.3. Separation of pre-event and event water

The separation of the hydrograph into water contributing from an occurring rainfall event (“event water”) or water stored in the ground prior to this event (“pre-event water”) is important for the understanding of geochemical processes taking place in the soil. Therefore, for geochemical modeling it’s important to know when and how much event and pre-event water can be expected from different rainfall events. In rainfall – runoff analysis a hydrograph separation into event and pre-event can be done using environmental or artificial tracers for experiments.

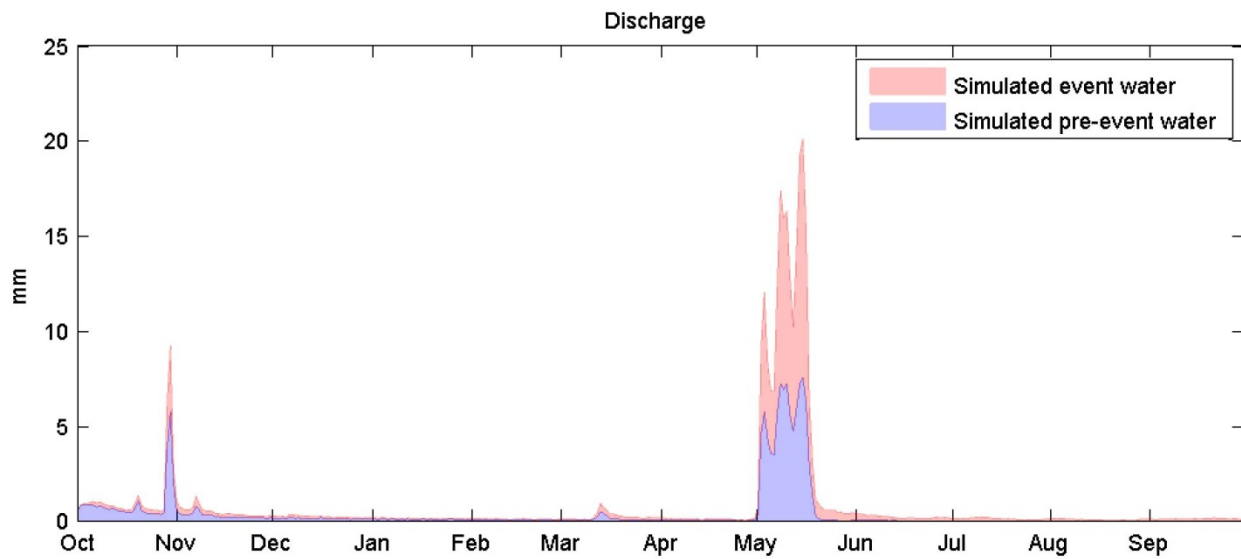


Figure 21: Hydrograph separation based on the amount of simulated old and new water particles for simulation Run(52/10)

The MIPS model also provides information about the amount of water with event and pre-event origin contributing to runoff (see Figure 21). Here simulation particles, which were pre-populating the slope at initial time, are labeled *old* or *pre-event* water - and simulation particles infiltrating the soil due to precipitation events during the considered time period were labeled *new* or *event* water. Since there exists no information from tracer experiments for the considered time period, the model performance in terms of predicting the amounts of event and pre-event water is subject to further investigation.

Although no tracer information exists for the investigated time period, information from earlier research (Bishop, 1991) and later research (Laudon, 2004) for the same experimental site can be used for first comparisons. Bishop (1991) estimated that the pre-event water fraction is about 91% of the total runoff throughout storm events. Laudon (2004) analyzed

oxygen 18 levels in melt water, soil water and runoff. He found that about 75% of the total runoff of the snowmelt period is pre-event water.

Analyzing simulation Run(52/10), MIPS predicted a pre-event water fraction of about 48% for the whole hydrological year studied, and about 43% for the spring flood event in May.

3.3. Groundwater level

The groundwater table depth is of special interest when separating the saturated from the unsaturated zone in a soil profile and can also be considered as an indicator of the overall model performance.

The groundwater table depths along the transect for simulation Run(70/4) are given in Figure 22. The initial groundwater level at the start of the simulation period is equal for all locations. During the simulation period due to rainfall events, given soil properties and the occurrence of preferential flow pathways, the groundwater levels at different locations develop differently. After the initial stage the simulated groundwater levels were rising at location S22, S40 and S64 and falling at location S4 and S12. Furthermore it was found that the groundwater levels stabilized after the first month of the simulation period. Observed groundwater level data was available from manual observations for the considered time period but could also be recalculated from stream runoff – groundwater level relationships.

The dots in Figure 22 indicate the observed groundwater levels for the different locations. Comparing those with the results from the simulation it can be seen that the observed conditions could not be properly predicted. In fact, the ground water levels for all locations were over-predicted beside location S4 in November.

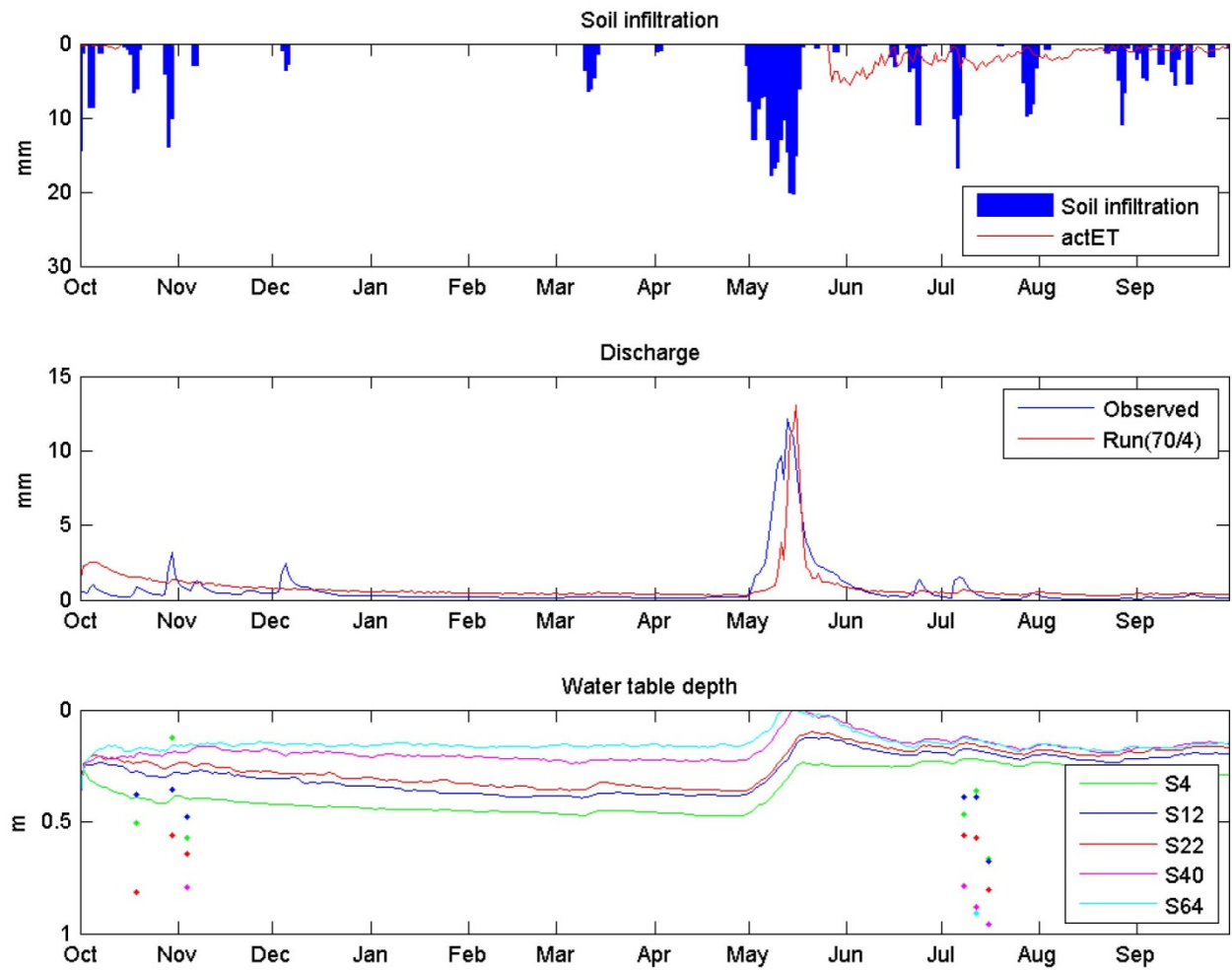


Figure 22: Groundwater table depths of simulation Run(70/4) for location S4, S12, S22, S40 and S64

To determine which parameter combination gives the best simulation performance in terms of predicting groundwater levels the simulated and observed groundwater levels of location S22 for all runs are depicted in Figure 23.

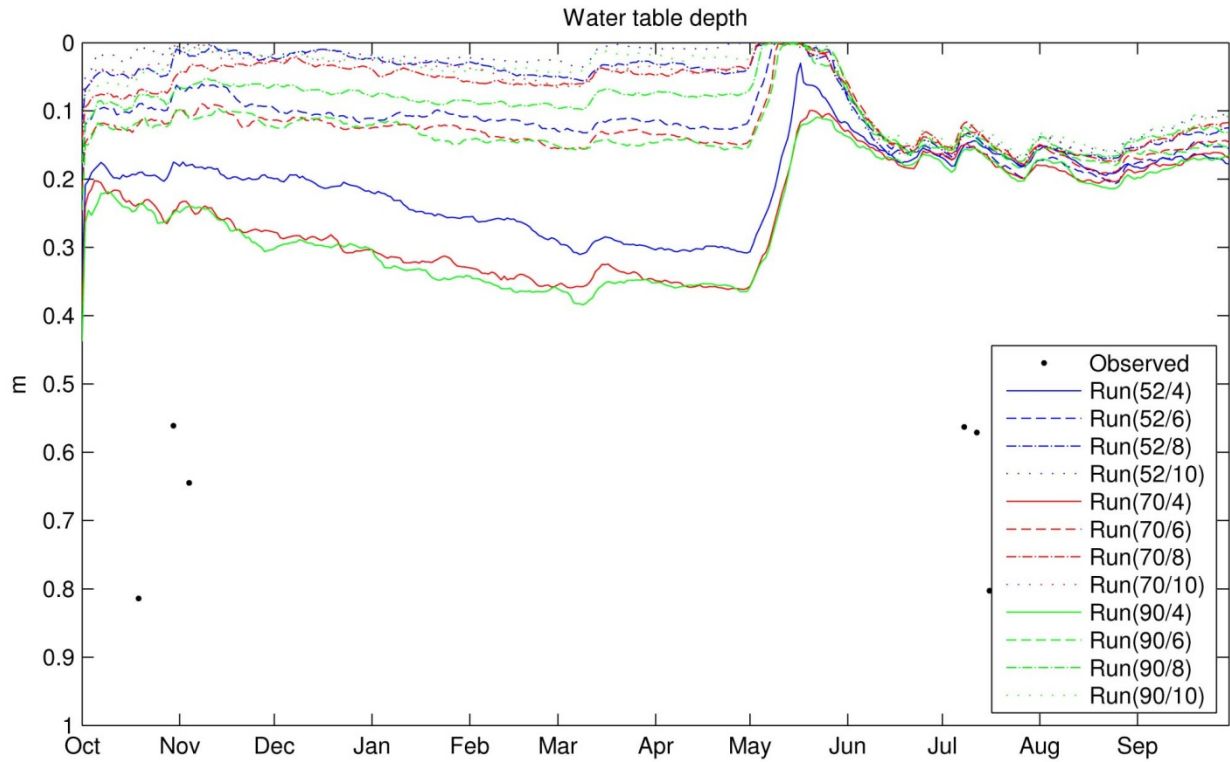


Figure 23: Groundwater table depths of all simulated runs for location S22

It can be seen that all simulated groundwater table depths were much smaller than the observed ones. The influence of the f -value on the groundwater level is much more significant than the influence of K_0 . In general it was found that by decreasing f and increasing K_0 the groundwater table depth could be increased.

3.4. Water storage

Similar to groundwater levels the amount of water that can possibly be stored is related to porosity. The amount of water that actually is stored within a slope is related to soil properties, rainfall events and slope geometry. The total water storage consists of water located in the unsaturated and saturated zones of a soil. Figure 24 summarizes the total water storage for all parameter combinations used in the simulations.

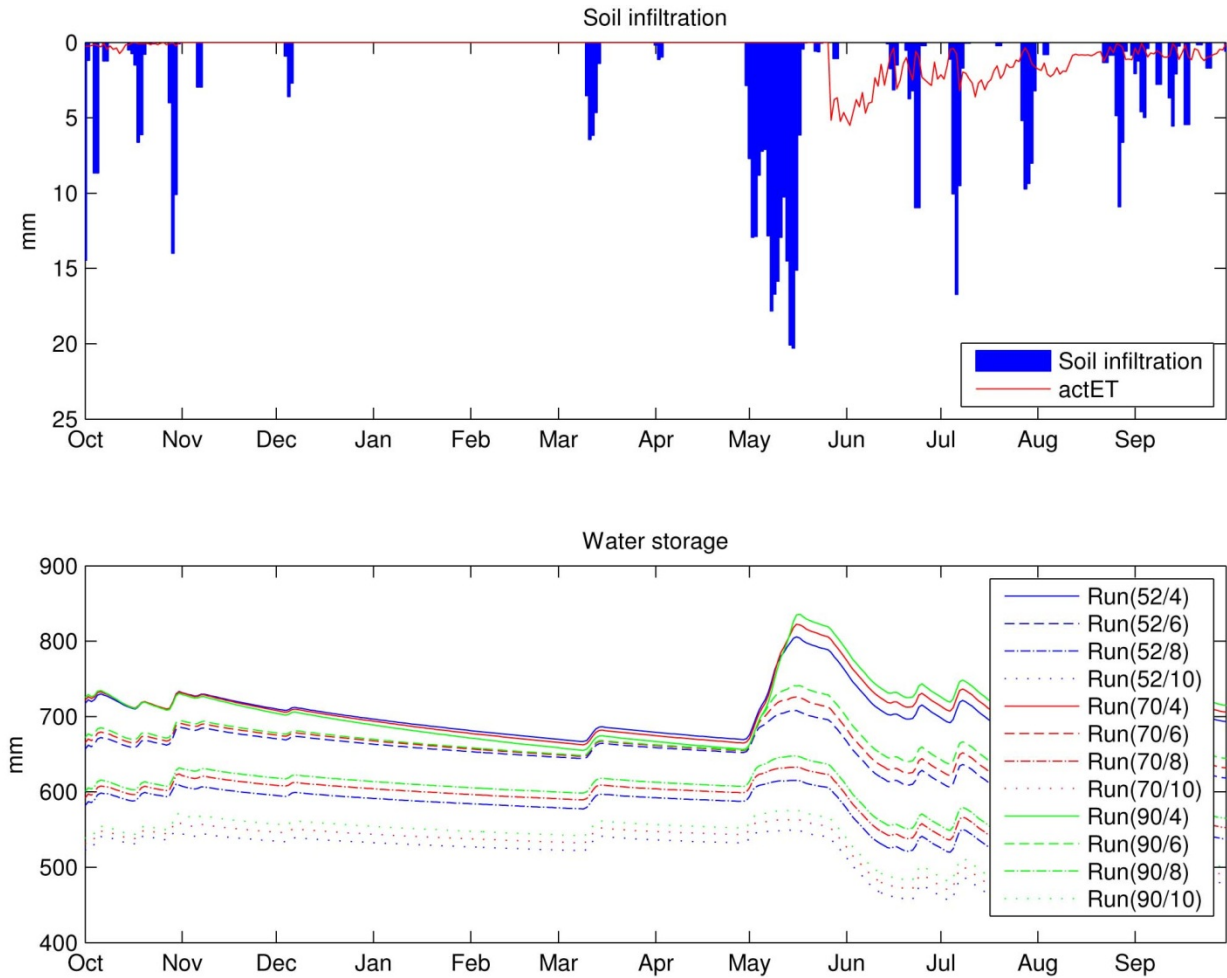


Figure 24: Daily soil infiltration and total water storage within the slope for all considered parameter combinations

Comparing the different simulation runs it was found that the amount of water stored within the slope generally increases with decreasing f and increasing K_0 . This can be explained with the changes in the porosity profile for different parameter combinations (see Figure 16b). Most available pore space and consequently also water storage was simulated for simulation Run(90/4) where the highest K_0 and lowest f -value were used.

During a MIPS simulation every particle's properties, like current position or velocity, can be stored for each time step. Using this information every particle can be identified whether it's located above or beneath the groundwater table. Particles located above the groundwater table can then be labeled as unsaturated zone water or if they are located beneath the groundwater table as saturated zone water. The amount of particles can always be converted into other units for every time step.

A water storage time series for the considered time period is shown in Figure 25. The red lines indicate the time steps at which particle properties like position or velocity were stored in the

simulation. From the time series it can be seen that from October to May the amount of water stored in the unsaturated zone doesn't change much. From May onwards due to spring runoff and precipitation events the water storage changes significantly.

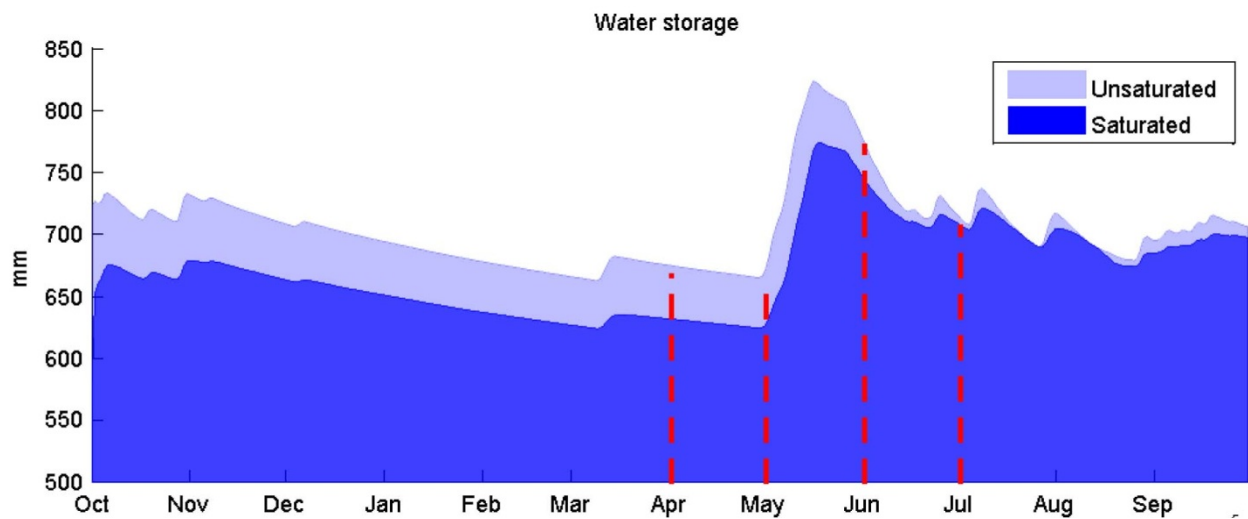


Figure 25: Water storage in the unsaturated and saturated zone for simulation Run(70/4)

As mentioned earlier, the MIPS concept allows storage of the position of every water particle at any time step. In Figure 26 snap-shots of the transect with water particles in the unsaturated and saturated zone, water tables and evapotranspired water particles are plotted for the beginning of April, May, June and July 1997 (see also Figure 25).

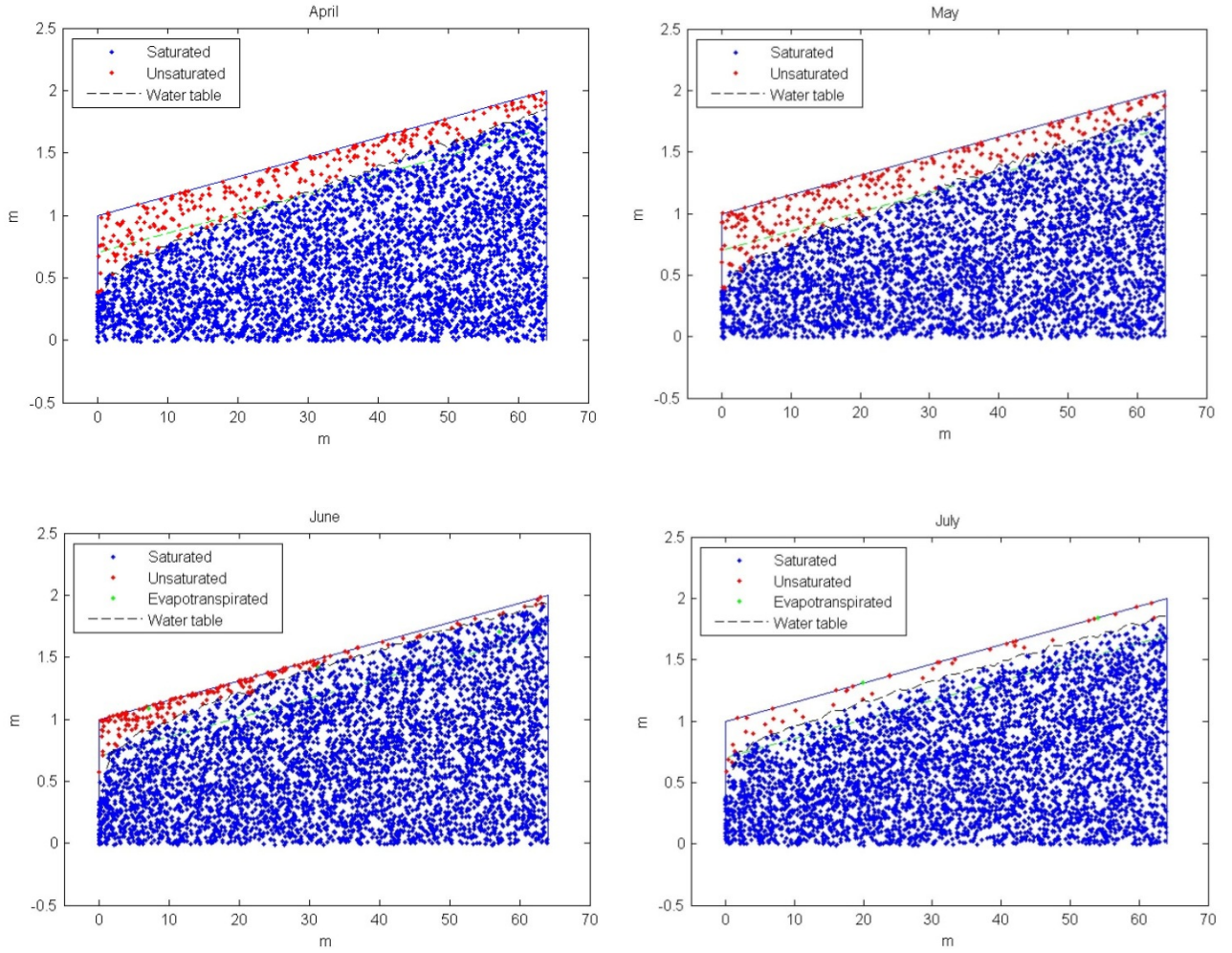


Figure 26: Water particles evapotranspired and stored in the unsaturated and saturated zone for the time steps at the beginning of April, May, June and July 1997 of simulation Run(70/4)

Comparing Figure 25 and Figure 26 some correlations have been found. In the months April and May more water is stored in the unsaturated zone than in the other months June and July. The smallest amount of water particles in the unsaturated zone were found in July. Even though the water table is comparatively low at that time step no precipitation occurred some days before and therefore less water particles are present in the unsaturated zone. Evapotranspired water particles appear only in June and July – as there was no actual evapotranspiration taking place before the middle of May.

3.5. Evapotranspiration

In this work, probability transition matrices were used to incorporate the effect of evapotranspiration into the MIPS concept. A linear decrease of particles availability for evapotranspiration from the ground surface to the rooting depth was assumed. Figure 27 illustrates this linear decrease of evapotranspired water particles with depth.

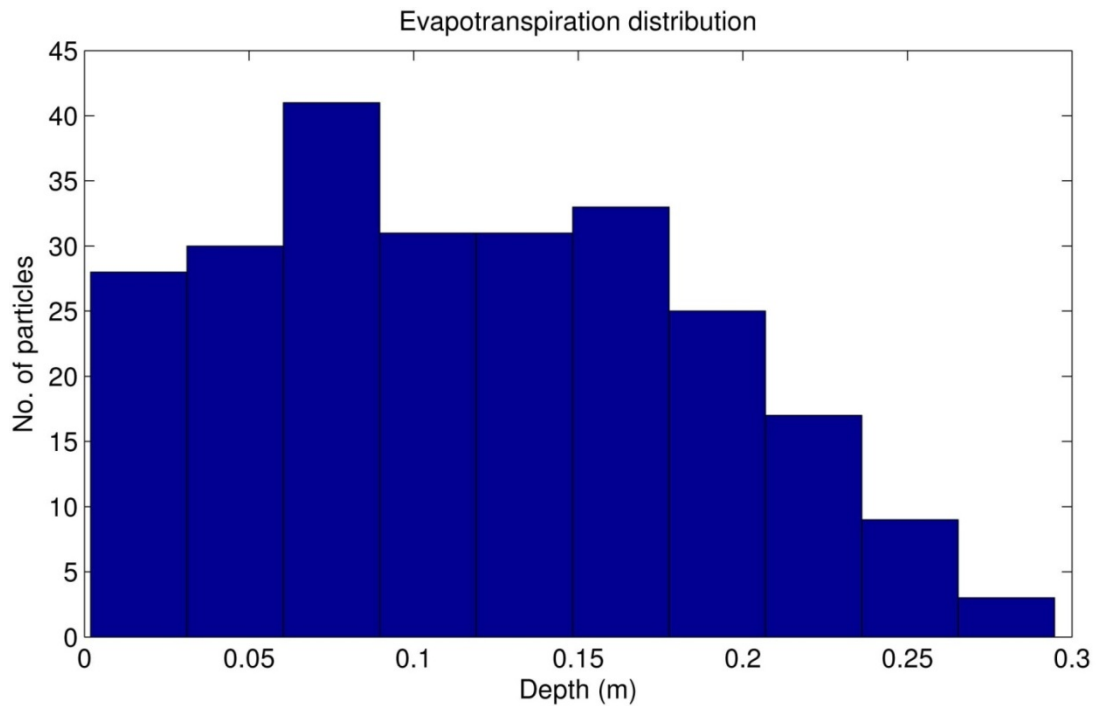


Figure 27: Number of particles for evapotranspiration stored at different depths at the beginning of June 1997 of simulation Run(70/6)

The amount of water particles at rooting depth level of 0.3 m is 0. Then it linearly increases until a depth of 0.15 m. From the depth of 0.15 m to the ground surface a linear increase could no longer be observed. The highest actual evapotranspiration rate was observed in the beginning of June. It can therefore be assumed that the amount of particles for evapotranspiration never exceeded the amount of particles available for evapotranspiration during the studied time period.

Another way of explaining how and to which extent evapotranspiration was included into MIPS is to plot the transect including particles for evapotranspiration, the water table and the rooting depth. In Figure 28 it can be seen that no particles are chosen for evapotranspiration below rooting depth. Here, evapotranspired particles are not active in the slope, but are the final position of particles before they are removed via evapotranspiration. Furthermore, water particles were taken up by roots for evapotranspiration independently of the unsaturated or saturated zone of the slope.

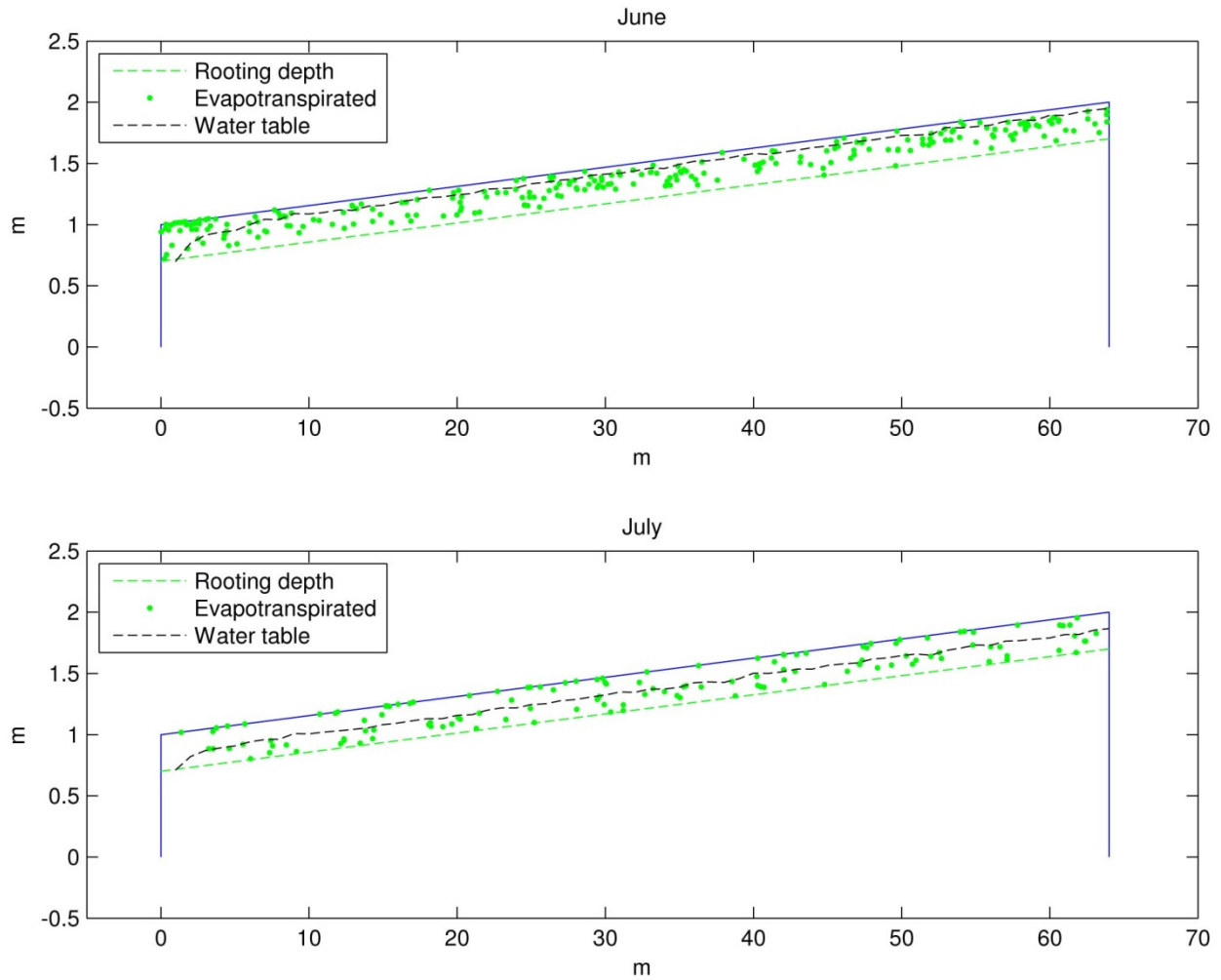


Figure 28: Water particles for evapotranspiration at the beginning of June and July 1997 in simulation Run(70/6)

3.6. Velocity distribution

In the MIPS concept velocities are assigned to each water particle located in the saturated zone according to an exponential distribution between a minimum and a maximum velocity. The minimum velocity was set to 0.0001 md^{-1} and the maximum velocity changes according to the saturated hydraulic conductivity profile (see Figure 13). In Figure 29 water particle velocities of particles located in between 0.5 – 0.7 m depth and 31 – 32 m length of the slope are illustrated using a histogram.

It was found that the decrease in particle velocities follows the exponential decrease assumption (see Figure 13). About 600 water particles have velocities between 0.0001 and 0.1 md^{-1} . Higher velocities were only simulated for a smaller number of particles.

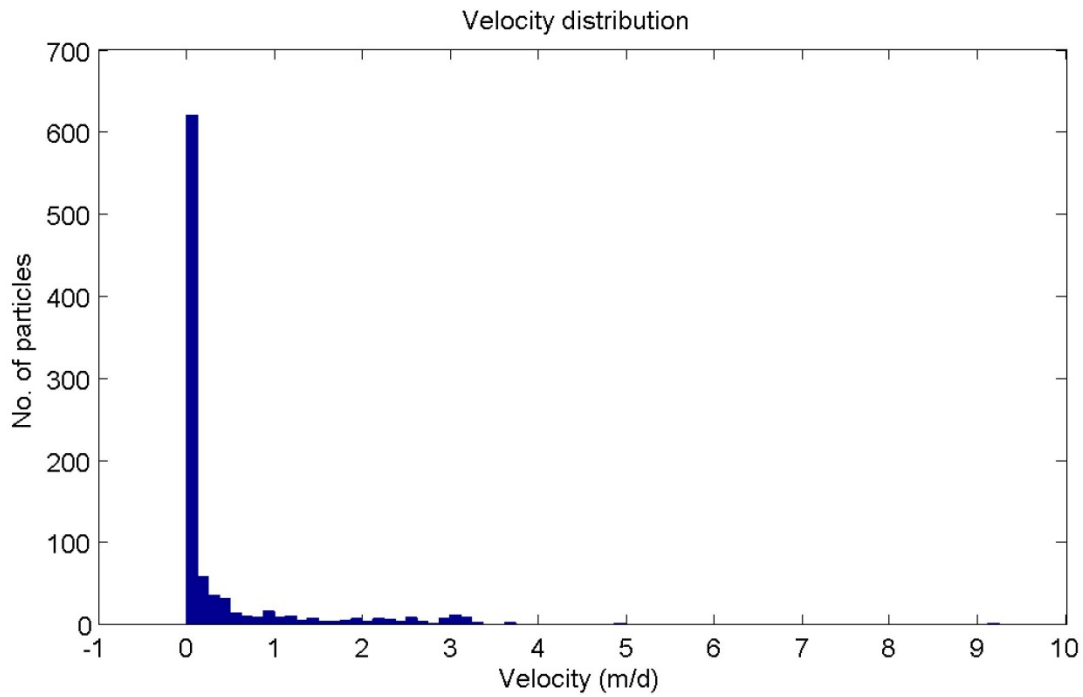


Figure 29: Number of particles within different velocity ranges in simulation Run(70/6)

The histogram above only illustrates the assigned water particle velocities for a certain small area of the slope. Another representation of particle velocities for the whole slope was done by introducing velocity classes and plotting water particles according to those classes (see Figure 30).

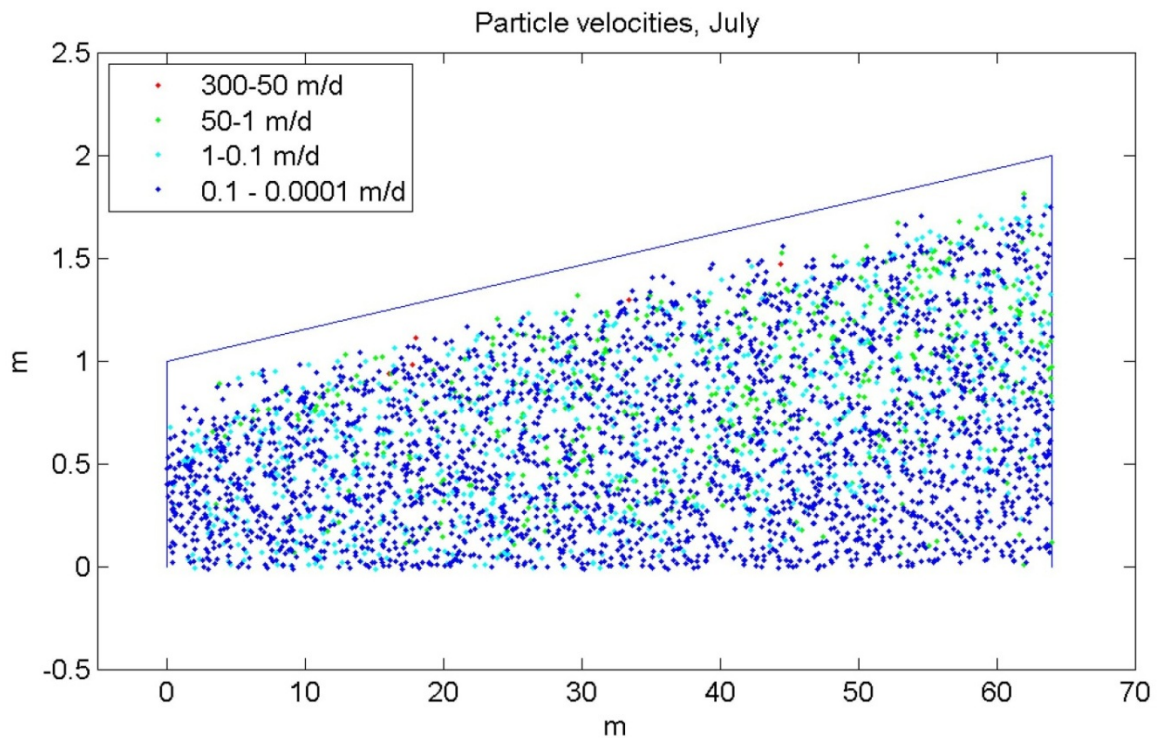


Figure 30: Water particle velocities at the beginning of July 1997 of simulation Run(70/6)

In Figure 30 only particle velocities of water particles located in the saturated zone are depicted. It was found that in correlation with the exponential decrease function higher particle velocities of 1 to 300 m/d (green and red color) were mainly found close to the ground surface. Low particle velocities of 0.0001 to 1 m/d (blue and cyan color) were found to occur all over the slope.

3.7. Unsaturated zone initial flux

One underlying assumption of the MIPS concept is that at initial time the slope is in steady state condition which means that the amount of water entering the system is equal to the amount of water exiting the system. To test if this initial condition assumption is adequate for simulating short period simulation outputs like discharge, the water storage and groundwater levels were compared with long period simulation outputs.

For the short period runs one hydrologic year was chosen starting in October 1996. The initial input flux from the unsaturated zone was assumed to be the same as the slope's discharge at the same initial time step. Usually, in hydrologic modeling, dry seasons are chosen for the start of simulations. At the beginning of October 1996 several rainfall events took place which led to discharges larger than predicted during the first month of the short period simulations. Compared to this in long period simulations the peaks in October were under predicted but still give better results (see Figure 31).

After the high amount of water of the short period simulation at initial time was drained both hydrographs give similar results, comparable to the observed discharge during January to May. During the spring flood from beginning of May to June both the long period and short period simulations were over predicting the observed peaks but vary only slightly from each other. After the main spring runoff event both simulated hydrographs give more or less equal results.

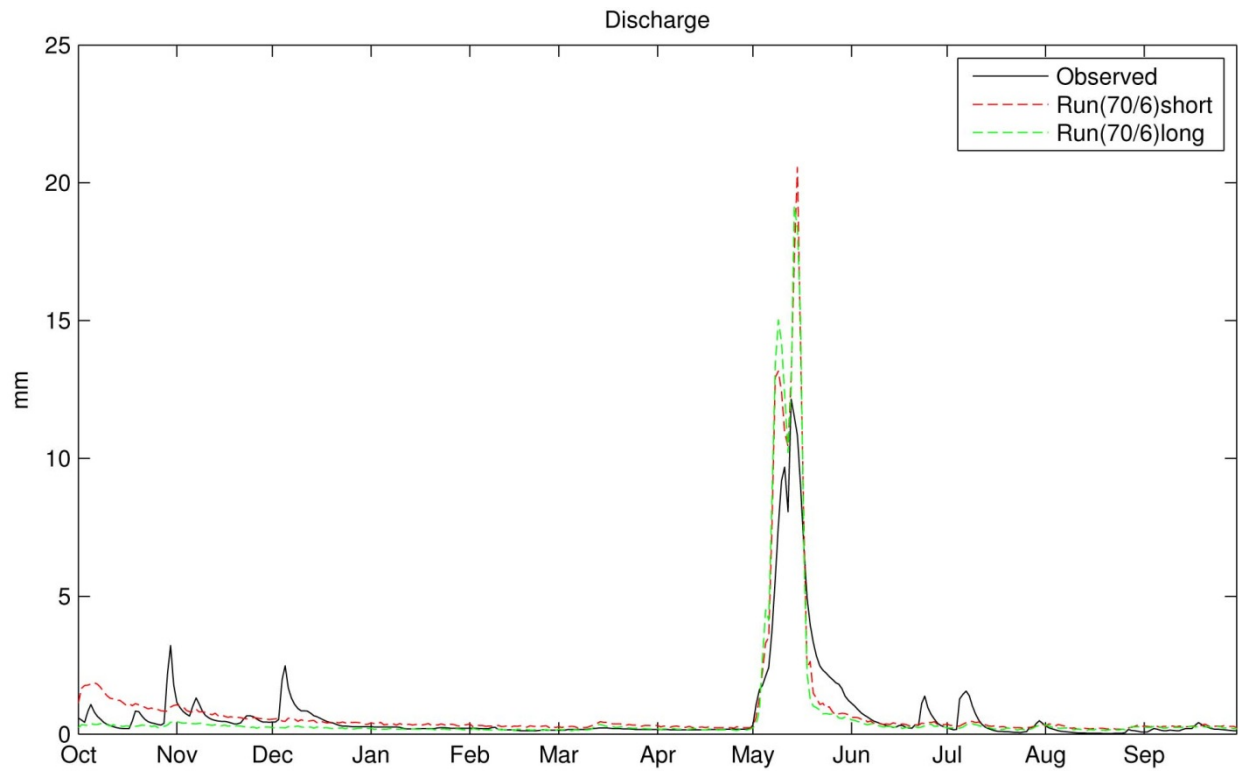


Figure 31: Hydrographs of the short and long period simulation of simulation Run(70/6) and observed data

The assumption that at initial time too much water flows into the system can also be discussed having a closer look towards groundwater levels and water storage. In terms of groundwater levels, the short period simulations predicted higher water tables during October to February and lower water tables from June to the end of September as compared to the long period simulation. From February to June both simulation period results were similar to each other (see Figure 32).

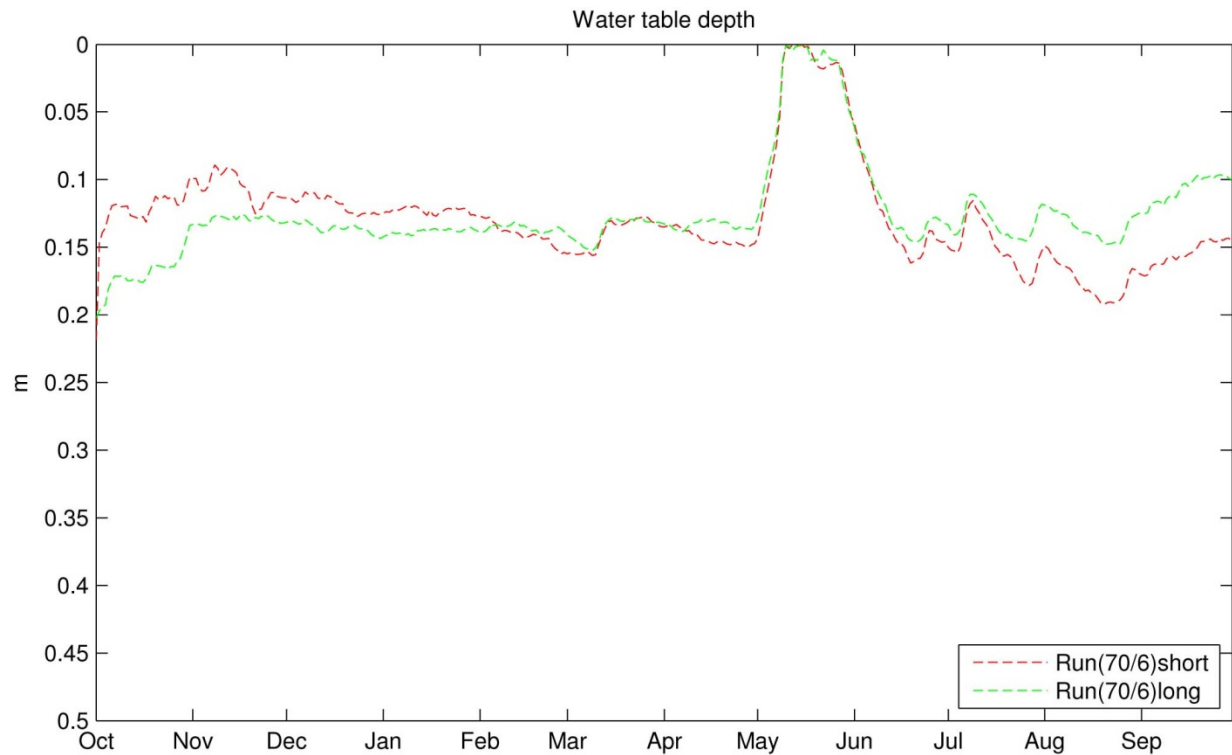


Figure 32: Water table depths of the short and long period simulation of simulation Run(70/6)

Since the groundwater levels and water storage within the slope are closely related to each other also the simulation outputs give similar results. While the short period simulation outputs of total water storage were higher from October to May - compared to the long period simulation - they were lower from August to the end of September and almost equal from May to August (see Figure 33).

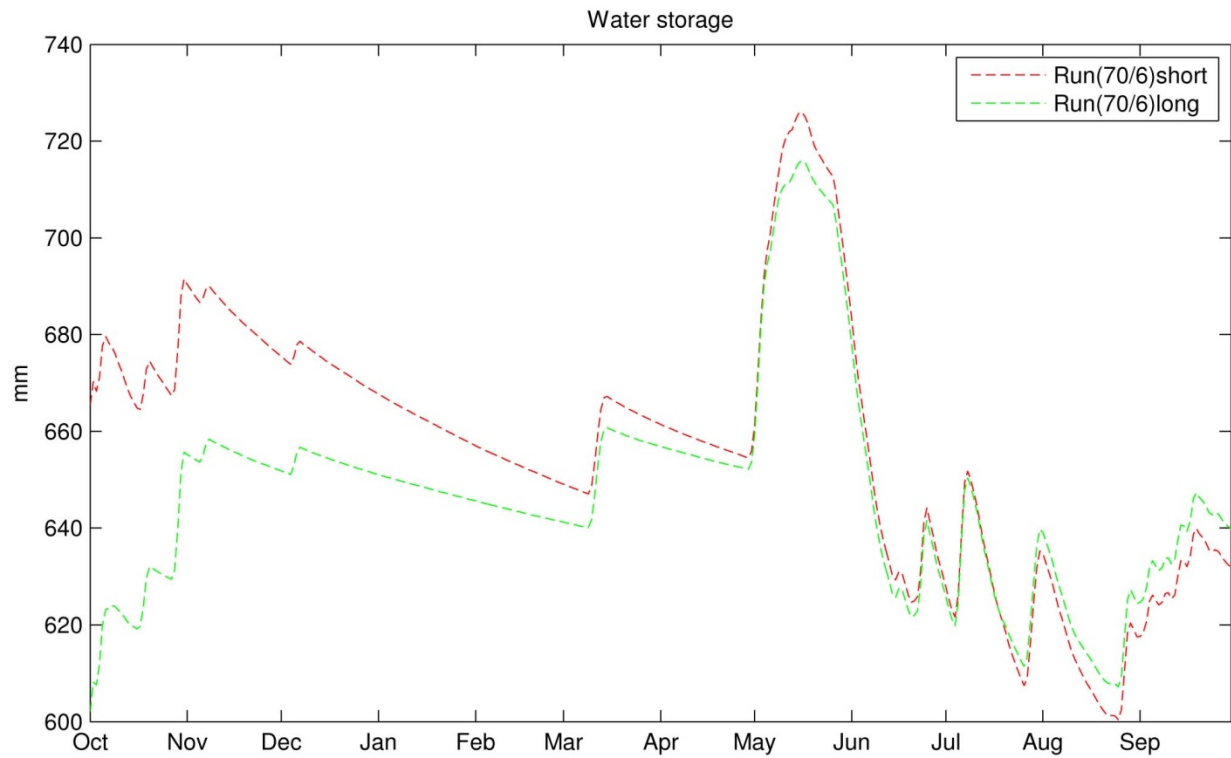


Figure 33: Water storage of the short and long period simulation of Run(70/6)

3.8. Slope geometry

To get the best and most realistic performance from MIPS simulations, the slope geometries have to be well known and must be approximated to real world conditions. To examine to which extent the model performance and the prediction of ground water tables or water storage changes, a MIPS simulation was conducted for a slope with a different geometry than the ones for the previous simulations. The simulation run with the best model performance (Run(52/4)) was found the most appropriate for comparisons in terms of model performance. Basically only the slope length and angle were altered which resulted in different soil depths (see Table 4).

Table 4: Slope geometry relevant parameters for simulation Run(52/4) and Run(52/4)90

Parameter	Units	Run(52/4)	Run(52/4)90
Slope length	m	64.00	90.00
Slope width	m	10.00	10.00
Soil depth	m	1.0 - 2.0	1.0 – 5.0
Slope angle	deg	1.72	2.54

Even though the simulated runoff was slightly higher for simulation Run(52/4)90 from October to May the higher prediction of the first peak of the spring runoff event gave better results (see Figure 34). After the spring runoff event both simulation hydrographs were almost equal to each other. The overall model performance was better for simulation Run(52/4)90 where the error variance was 0.52 and the efficiency was 0.79.

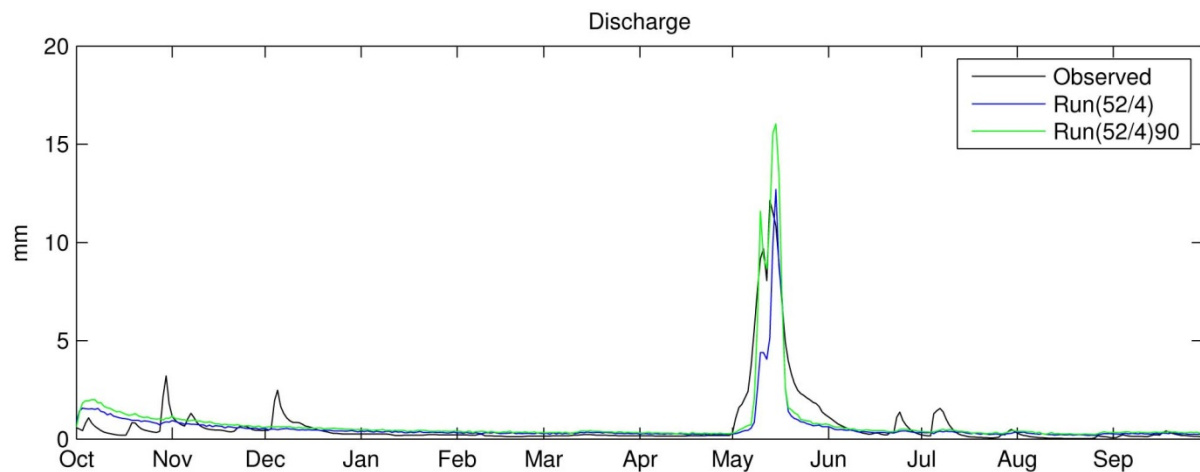


Figure 34: Hydrographs of simulation Run(52/4), Run(52/4)90 and observed data

Similar to the results from the earlier simulations most groundwater levels were over-predicted by simulation Run(52/4)90 (see Figure 35). Comparing both simulations it was found that with changed slope geometries the groundwater levels at the different locations were lower, except for location S40. Therefore the simulated lower groundwater levels are assumed to be more realistic.

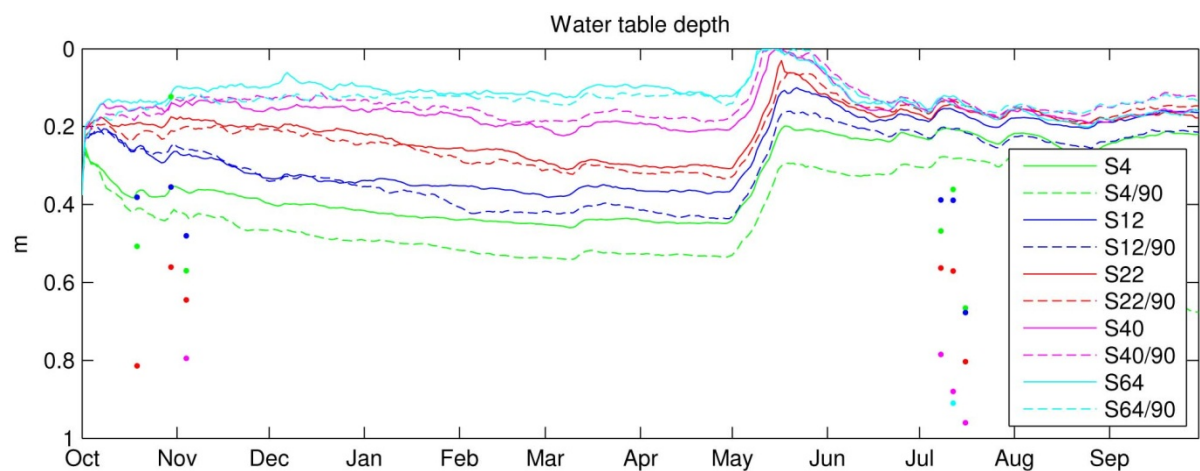


Figure 35: Water table depths of simulation Run(52/4), Run(52/4)90 and observed data for all locations

In the MIPS concept a change in geometry has probably the highest influence on the simulated water storage. In Figure 36 it can be seen that the predicted amounts of water storage for simulation Run(52/4)90 are about 400 mm higher throughout the simulated time period while the change in water storage over time is more or less identical.

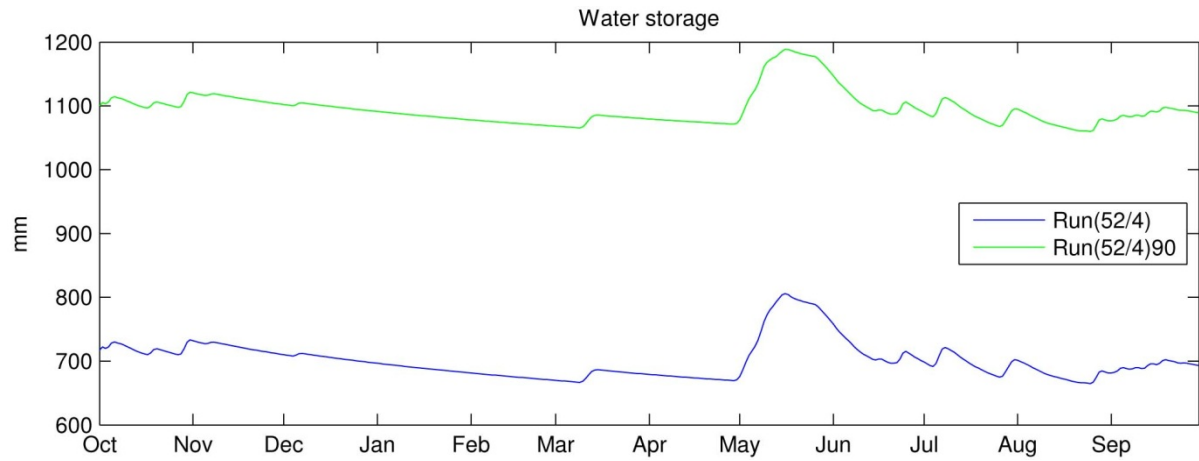


Figure 36: Water storage of simulation Run(52/4) and Run(52/4)90

4. Discussion

In the following chapter the problems stated in the introduction of this work will be discussed. Some key points for understanding the MIPS model are the runoff – groundwater level relationships, where soil types with their different properties play an important role. Other fields of interest are groundwater table depth and water storage correlations, and how preferential flow pathways and probability transition matrices are applied in the model. As a starting point, the overall performance of the model, and the method used for its estimation, is analyzed.

4.1. Goodness – of – fit

Even though the sum of squared errors and efficiency of Nash and Sutcliffe is not an ideal measure for the goodness – of – fit estimation of a rainfall – runoff model it was found to be sufficient for the purpose of this work. Beven (2012) stated three reasons why the usage of this still widely used performance measure should be reconsidered by hydrologic modelers. Besides the effect of giving greater weight to predictions near the hydrograph peaks by squaring the errors and sensitivity towards timing errors, the residuals may also be auto-correlated in time.

Other measures that could be applied for estimating the performance of MIPS are based upon Bayesian statistics; there likelihood functions, prior and posterior distributions for the parameters are combined to estimate the probability of predicting a new observation (Beven, 2012).

Comparing the error variance and the efficiency estimates of the short period simulations with those of the long period simulations, it can be seen that the long period simulations give a better overall performance of the model for higher f-values and a worse performance for lower f-values. This can be explained with the higher or lower differences in the hydrograph outputs for different parameter combinations, compared to observed data, and the influence of badly chosen initial conditions. Furthermore, almost no high peaks were observed during the first half of the long period simulations which also result in a lower error variance since high peaks were often over predicted by the model. The timing of the simulated and observed peaks was found to coincide well for both the short and long period simulations. Therefore, timing errors played a less important role for differences in the estimated performance.

Another way to illustrate which parameter combination fits best, is to draw parameter response surfaces with goodness-of-fit represented as contours. Since only 12 different parameter combinations were tested in this work it was not possible to draw response surfaces where more parameter combinations are needed.

4.2. Transmissivity feedback and discharge

Surface saturated hydraulic conductivity – and a parameter for its decrease with depth, the f -value – were found to have the largest influence on the simulated hydrographs. The way the hydrographs reacted towards changes of those two parameters can be explained by the ‘transmissivity feedback theory’.

Since the transmissivity in MIPS is defined as the integral over the conductivity function from soil depth to water table depth, every change in the conductivity function changes the transmissivity of the soil. Hence, transmissivity increases with decreasing f -value and increasing surface saturated hydraulic conductivity. A higher soil transmissivity means that more water drains towards the stream which is the explanation for the over predicted base flow in winter. On the other hand by decreasing the f -value the system becomes less sensitive for predicting hydrograph peaks. This can be explained by more gradual changes in hydraulic conductivity with depth for a low f -value, as compared to more abrupt changes for high f -values.

In terms of hydrograph separation, the MIPS model outputs could be used to prove the theory that pre-event water is strongly contributing to stream runoff during and after big rainfall events. First comparisons in terms of model performance have been done using information from measured 18O experiments conducted at the same experimental site (Bishop (1991) and Laudon (2004)). As compared to the ones estimated from measured 18O it was found that the MIPS predictions underestimated the amount of pre-event water contributing to runoff during high spring runoff and storm events. More detailed comparisons have been postponed for later work because of lack of proper tracer data for the chosen simulation period which could have been used as a good reference for performance measures. Likewise, the influence of groundwater stored in deeper layers than the slope geometries comprise should be further examined.

4.3. Groundwater levels and water storage

From comparisons of predicted and observed groundwater level data, it was found that none of the chosen parameter combinations was able to give reasonable results. One reason for that could be the fact of different soil types. Since both the measured porosity and hydraulic conductivity profiles are very different for both the near stream peat and the more distant till soil, it will be difficult to find one proper parameter combination which gives reasonable simulation outputs in terms of groundwater levels. The importance, which different soil types might have, should be further investigated by dividing the slope into vertical segments exhibiting those individual properties of each soil. The introduction of different soil types could be done within the MIPS concept.

Another reason why the observed groundwater levels were not met by the simulations can be found in the realization of the MIPS concept itself. The concept assumes a linear relationship of porosity decrease with depth to recalculate the groundwater table depths along the slope. This assumption might be valid for shallow soils where a theoretical porosity of 0 or 1 is never reached, but might be wrong for deeper soil profiles where a theoretical porosity of zero might be reached and therefore the water tables are simply calculated upon an incorrect starting depth. In practice, it isn't possible to measure porosities lower than zero and higher than one and although the soil layer at the S-Transect is several meters thick, the porosity never drops below a certain value or reaches the value 0. Choosing a different relationship which fits the measured data better would probably also give more realistic results.

Even though no realistic groundwater levels were simulated, some interrelations of groundwater table depths and water storage produced by the MIPS model were identified. Specifically, these are the finding that high f -values simulate low groundwater levels; but also: low groundwater storage can be explained according to the steeper decrease in the porosity profile. Lower f -values allow higher water storage because of the resulting higher porosities and therefore higher storage volumes. Since the water table depth is recalculated according to the porosity profile, higher storage volumes result in lower groundwater levels.

Besides altering the f -value, the changes in the slope's geometry have been found an important factor for the correct representation of groundwater levels and water storage. One finding was that lower groundwater levels could be achieved using a steeper and longer slope which gave increased soil depths. Especially, the amounts of predicted water storage changed considerably due to the increase in storage volume resulting from larger soil depths. The big differences to water storage predictions from other models (e.g.: max. 350 mm COUP model

result, Stähli et al, 2001) can also be explained with the difference in the initial slope geometries for the simulations. In the conducted MIPS simulations deeper soil profiles with a higher possible storage volume depending on the porosity decrease with depth relationship were chosen, while the COUP model simulated the liquid water storage only for the upmost 45 cm of the soil profile.

Once the groundwater levels are correctly simulated, the MIPS model allows the slope to be divided into a saturated and unsaturated zone. To examine to which extent the model is capable of predicting the amounts of water stored in the different zones correctly, more analysis will be necessary.

4.4. The influence of evapotranspiration

Early MIPS simulations on the S-Transect were conducted without including the water loss due to evapotranspiration. This led to predicted peaks far too high, primarily after the spring runoff event, when evapotranspiration influences the water balance in this region. The inclusion of evapotranspiration into MIPS led to under-predicted peaks for the same time period. Since the actual evapotranspiration data used was estimated by the HBV model according to the water balance, the main reasons why the hydrograph was under-predicted are probably the same as the ones discussed for runoff.

As in other instances, the transition probability matrix used was assuming a linear decrease in particles available for evapotranspiration from soil surface to rooting depth. A good illustration of this relationship couldn't be established because the amount of water needed for evapotranspiration never exceeded the amount of water stored in the soil. More information should be obtained at times when the evapotranspiration demand is maximal - and less water is stored in the soil.

4.5. Particle velocities and their representation

Individual velocities were assigned to each water particle according to an exponential function depending on its position within the slope. For representation purposes, not the particles at a certain soil depth, but the soil volume was analyzed. Due to the effects of randomness not enough particles were found at a single soil depth to illustrate the exponential relationship.

Furthermore, higher particle velocities were simulated for locations closer to the slope's surface. This finding corresponds well with the decrease of hydraulic conductivity with depth.

Another possibility to illustrate the representation of velocities would be to divert the occurring velocities into classes and plot the amount of particles for each class with depth.

4.6. The steady state assumption

By comparing a short period run with a long period run the steady state at initial time assumption was analyzed. The fact that rainfall occurred right at the initial time step, probably led to an over-prediction in the simulated discharge, groundwater levels and water storage. This over-prediction would probably have been smaller if the beginning of the simulation had been in a dry season, without high precipitation events, or, as in the case of the long period simulation, assuming dynamic conditions and smaller unsaturated zone initial flux.

5. Conclusion

According to the aim stated in the introduction, several key issues for applying the MIPS model have been investigated. Soil properties have been found of great importance for the model performance in terms of runoff-, groundwater level- and water storage prediction. Especially soil porosity measurements are a reliable basis for the estimation of relevant model input parameters.

The model was able to predict the timing and peaks of the discharge hydrograph with reasonable success. Groundwater levels and consequently water storage was not well simulated for most of the parameter combinations. It was found that different soil types and simplified assumptions like the recalculation of groundwater levels according to a linear relationship are the primary reason for that.

Furthermore, the steady state assumption led to more runoff at the beginning of the simulation period. By running the simulation for longer time periods, dynamic conditions have been tested which brought significantly better results.

In this work a transition probability matrix was used to incorporate evapotranspiration into the model. The effect was, that over-predicted hydrograph peaks for runoff could be corrected – which leads to better model performance.

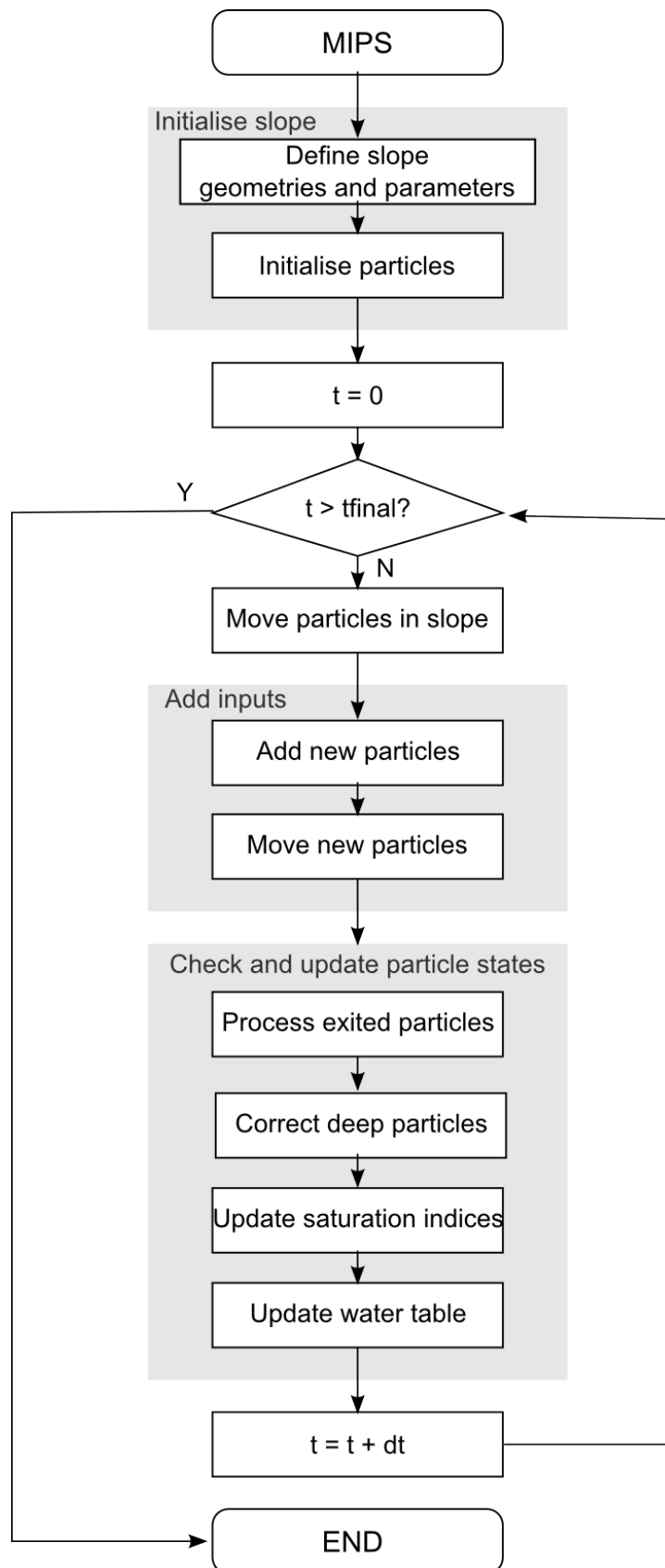
Further research should focus on the effects of different soil types within a slope on the model performance. Simplified assumptions, like steady state condition at initial time and linear decrease of porosity with depth, should be further investigated and alternatives considered.

Even though many assumptions were made, the MIPS model proves to be a valuable tool for understanding and simulating groundwater flow and opens new approaches to account for soil heterogeneity and preferential flow pathways.

Acknowledgements

I would like to express my deepest gratitude to my supervisors Kevin Bishop and Josef Fürst for providing me with all necessary facilities, equipment and expertise requested. Furthermore, I would also like to thank Jessica Davies for her invaluable guidance, support and motivation throughout my research. Many thanks are also due to Keith Beven and Jan Seibert for their advice during my research and my father Stephan Tschiesche for fine tuning the language of this paper.

Appendices



Appendix 1: Flow chart of the MIPS model (from Davies, 2011)

Register of Figures

Figure 1: a) Location of the catchment and b) the studied hillslope within the catchment (from Laudon, 2004).....	5
Figure 2: Overview of measurement locations along Västrabäcken and the S-transect (after Bishop, 1993)	6
Figure 3: Daily soil infiltration, discharge and air temperature during the investigated time period.....	8
Figure 4: Groundwater table depth – Discharge relationship at different locations along the S-transect. The lines represent the logarithmic relationship	10
Figure 5: Actual evapotranspiration estimates from the HBV model during the investigated time period.....	10
Figure 6: The S-Transect with soil type information, minimum and maximum measured groundwater levels from manual observations and instrumentation (Lysimeter, Piezometer, TDR, Temperature probes, Soil gas probes, Groundwater tubes) locations (from Bishop, 1993)	11
Figure 7: a) Saturated hydraulic conductivity profile and exponential regression relationship for location S4, S12 and S22; b) Porosity profile and linear regression relationship for location S4, S12 and S22 (after Nyberg, 2001).....	12
Figure 8: Slope geometries and basic model assumptions	14
Figure 9: a) Assumed saturated hydraulic conductivity profile (after Stähli, 2001) with exponential regression relationship; b) Derived porosity profile with parameters: $K_0 = 52$ m/day; $f = -10$; $v_0 = 0.0001$ m/day and $b = 25$ and linear relationship from soil samples for location S4, S12 and S22	16
Figure 10: Slope profile showing step size, unsaturated and saturated zone	18
Figure 11: Slope profile with recharge from the unsaturated zone, initial upslope- and lateral flux.....	18
Figure 12: Slope profile with water table depth, soil depth and water storage in the saturated zone.....	20

Figure 13: Representation of how velocities are assigned according to an exponential distribution between a minimum and maximum velocity and Equation 3 (from Davies, 2011)	20
Figure 14: Slope profile with schematic particle movement	22
Figure 15: Slope profile with evapotranspired particles, particles in the unsaturated and saturated zone	24
Figure 16: Set of K_0 and f combinations used for running the MIPS model	27
Figure 17: Daily soil infiltration, actual evapotranspiration and predicted versus observed hydrographs for simulation Run(52/10)	30
Figure 18: Observed and predicted hydrographs for all considered parameter combinations	31
Figure 19: Observed and predicted hydrographs for simulations with changing surface saturated hydraulic conductivity and $f = 8$	32
Figure 20: Observed and predicted hydrographs for simulations with changing f -values and $K_0 = 52$	33
Figure 21: Hydrograph separation based on the amount of simulated old and new water particles for simulation Run(52/10)	34
Figure 22: Groundwater table depths of simulation Run(70/4) for location S4, S12, S22, S40 and S64	36
Figure 23: Groundwater table depths of all simulated runs for location S22	37
Figure 24: Daily soil infiltration and total water storage within the slope for all considered parameter combinations	38
Figure 25: Water storage in the unsaturated and saturated zone for simulation Run(70/4)	39
Figure 26: Water particles evapotranspired and stored in the unsaturated and saturated zone for the time steps at the beginning of April, May, June and July 1997 of simulation Run(70/4)	40
Figure 27: Number of particles for evapotranspiration stored at different depths at the beginning of June 1997 of simulation Run(70/6)	41
Figure 28: Water particles for evapotranspiration at the beginning of June and July 1997 in simulation Run(70/6)	42

Figure 29: Number of particles within different velocity ranges in simulation Run(70/6).....	43
Figure 30: Water particle velocities at the beginning of July 1997 of simulation Run(70/6) ..	43
Figure 31: Hydrographs of the short and long period simulation of simulation Run(70/6) and observed data	45
Figure 32: Water table depths of the short and long period simulation of simulation Run(70/6)	46
Figure 33: Water storage of the short and long period simulation of Run(70/6)	47
Figure 34: Hydrographs of simulation Run(52/4), Run(52/4)90 and observed data.....	48
Figure 35: Water table depths of simulation Run(52/4), Run(52/4)90 and observed data for all locations.....	48
Figure 36: Water storage of simulation Run(52/4) and Run(52/4)90	49

Register of Tables

Table 1: Maximum and minimum groundwater table depths from manual observations along the transect between 1996 to 1998	9
Table 2: Parameters required by the MIPS model (Run(52/10))	26
Table 3: Error variance and efficiency after Nash and Sutcliffe (1970) for all conducted short period and long period MIPS simulations	29
Table 4: Slope geometry relevant parameters for simulation Run(52/4) and Run(52/4)90	47

References

- Beven, K. Changing ideas in hydrology — The case of physically-based models. *Journal of Hydrology* 105(1), 157-172.
- Beven, K.J. Preferential flows and travel time distributions: defining adequate hypothesis tests for hydrological process models Preface. *Hydrological Processes* 24(12), 1537-1547.
- Beven, K.J. (2011). *Rainfall- Runoff Modelling: The Primer*. Hoboken: Hoboken : John Wiley & Sons.
- Bishop, K. (1991). *Episodic Increases in Stream Acidity, Catchment Flow Pathways and Hydrograph Separation*. Diss.:University of Cambridge.
- Bishop, K., Seibert, J., Nyberg, L. & Rodhe, A. Water storage in a till catchment. II: Implications of transmissivity feedback for flow paths and turnover times. *Hydrol. Process.* 25(25), 3950-3959.
- Davies, J., Beven, K., Nyberg, L. & Rodhe, A. A discrete particle representation of hillslope hydrology: hypothesis testing in reproducing a tracer experiment at Gårdsjön, Sweden. *Hydrological Processes* 25(23), 3602-3612.
- Ewen, J. ‘ SAMP’ model for water and solute movement in unsaturated porous media involving thermodynamic subsystems and moving packets: 1. Theory. *Journal of Hydrology* 182(1), 175-194.
- Hillel, D. (2004). *Introduction to environmental soil physics*. Amsterdam ; Boston: Amsterdam ; Boston: Elsevier Academic Press.
- Laudon, H., Hemond, H.F., Krouse, R. & Bishop, K.H. Oxygen 18 fractionation during snowmelt: Implications for spring flood hydrograph separation. *WATER RESOURCES RESEARCH* 38(11).
- Laudon, H., Seibert, J., Kohler, S. & Bishop, K. Hydrological flow paths during snowmelt: Congruence between hydrometric measurements and oxygen 18 in meltwater, soil water, and runoff. *WATER RESOURCES RESEARCH* 40(3).
- Lindstrom, G., Bishop, K. & Lofvenius, M.O. Soil frost and runoff at Svartberget, northern Sweden - measurements and model analysis. *Hydrol. Process.* 16(17), 3379-3392.
- McCuen, R.H. (1998), *Hydrologic Analysis and Design: Second Edition*. Pearson Education.
- Nyberg, L., Stähli, M., Mellander, P.-e., Bishop, K.H. & Mellander, P.-E. Soil frost effects on soil water and runoff dynamics along a boreal forest transect: 1. Field investigations. *Hydrological Processes* 15(6), 909-926.
- Price, J.F. (2006). Lagrangian and Eulerian Representations of Fluid Flow: Kinematics and the Equations of Motion. In. Woods Hole Oceanographic Institution.
- Reggiani, P. & Rientjes, T.H.M. Flux parameterization in the representative elementary watershed approach: Application to a natural basin. *WATER RESOURCES RESEARCH* 41(4).
- Rodhe, A. Flow paths of water in Swedish forests, I: Soil and surface water acidification in theory and practice. *Kungl. Skogs- Och Lantbruksakademins Tidskrift* 142(18), 23-29.
- Seibert, J., Bishop, K., Nyberg, L. & Rodhe, A. Water storage in a till catchment. I: Distributed modelling and relationship to runoff. *Hydrol. Process.* 25(25), 3937-3949.

- Seibert, J., Bishop, K., Rodhe, A. & McDonnell, J.J. Groundwater dynamics along a hillslope: A test of the steady state hypothesis. *WATER RESOURCES RESEARCH* 39(1).
- Seibert, J., Rodhe, A. & Bishop, K. Simulating interactions between saturated and unsaturated storage in a conceptual runoff model. *Hydrol. Process.* 17(2), 379-390.
- Stahli, M., Nyberg, L., Mellander, P.E., Jansson, P.E. & Bishop, K.H. Soil frost effects on soil water and runoff dynamics along a boreal transect: 2. Simulations. *Hydrol. Process.* 15(6), 927-941.